--Adeno-Associated Virus Gene Therapy Prevents Progression of Kidney Disease in Genetic Models of Nephrotic Syndrome

Authors: Wen Y. Ding[1], Valeryia Kuzmuk[1,6], Sarah Hunter[1], Abigail Lay[1**], Bryony Hayes[1***], Matthew Beesley[2], Ruth Rollason[1], Jennifer A. Hurcombe[1], Fern Barrington[1], Catrin Masson[1], William Cathery[1], Carl May[1], Jack Tuffin[6], Timothy Roberts[1], Geraldine Mollet[3], Colin J. Chu[4], Jenny McIntosh[5], Richard J. Coward[1], Corinne Antignac[3], Amit Nathwani[5], Gavin I. Welsh[1], Moin A. Saleem[1]*

Affiliations:

[1]Bristol Renal, Bristol Medical School, Dorothy Hodgkin Building, University of Bristol, Bristol BS1 3NY, UK.

[2]Department of Histopathology, Cheltenham General Hospital, Cheltenham GL53 7AN, UK.

[3] Laboratoire des Maladies Rénales Héréditaires, Inserm UMR 1163, Institut Imagine, Université Paris Cité, 75015 Paris, France.

[4]Academic Unit of Ophthalmology, Bristol Medical School, Biomedical Sciences Building, University of Bristol, Bristol BS8 1TD, UK.

[5]Research Department of Haematology, UCL Cancer Institute, Paul O'Gorman Building, University College London, London WC1E 6BT, UK.

[6]Purespring Therapeutics, Rolling Stock Yard, 188 York Way, London N7 9AS, UK.

* Corresponding Author:

Moin Saleem, M.Saleem@bristol.ac.uk Phone: 07775 801118

**Present address: Division of Cardiovascular Sciences, University of Manchester

***Present address: MRC Integrative Epidemiology Unit, University of Bristol, Bristol, UK

OVERLINE: KIDNEY DISEASE

One Sentence Summary: Adeno-associated virus gene therapy partially rescues function in genetic models of nephrotic syndrome both in vitro and in vivo.

Abstract: Gene therapy for kidney diseases has proven challenging. Adeno-associated virus (AAV) is used as a vector for gene therapy targeting other organs, with particular success demonstrated in monogenic diseases. We aimed to establish gene therapy for the kidney by targeting a monogenic disease of the kidney podocyte. The most common cause of childhood genetic nephrotic syndrome are mutations in the podocyte gene *NPHS2,* encoding podocin. We used AAV-based gene therapy to rescue this genetic defect in human and mouse models of disease. In vitro transduction studies identified the AAV-LK03 serotype as a highly efficient transducer of human podocytes. AAV-LK03-mediated transduction of podocin in mutant human podocytes resulted in functional rescue in vitro, and AAV 2/9 mediated gene transfer in both the inducible podocin knock-out and knock-in mouse models resulted in successful amelioration of kidney disease. A prophylactic approach of AAV 2/9 gene transfer before induction of disease in conditional knock-out mice demonstrated improvements in albuminuria, plasma creatinine, plasma urea, plasma cholesterol, histological changes and long-term survival. A therapeutic approach of AAV 2/9 gene transfer two weeks after disease induction in proteinuric conditional knock-in mice demonstrated improvement in urinary albuminuria at day 42 and 56 after disease induction, and corresponding improvements in plasma albumin. Therefore, we have demonstrated successful AAV-mediated gene rescue in a monogenic renal disease and established the podocyte as a tractable target for gene therapy approaches.

INTRODUCTION

Adeno-associated virus (AAV) is a small 20nm parvovirus that is predominantly episomal, has relatively low immunogenicity and transduces both proliferating and differentiated cells, making it an ideal vector for gene therapy. Gene therapy using AAV has seen many successes in targeting monogenic diseases in many organs, including hemophilia *(1–3)* for the liver, Leber's congenital amaurosis *(4)* for the eyes, and spinal muscular atrophy *(5)* for the neuromuscular system. AAV has shown effective transduction in these organs, and long-term gene expression has been seen beyond three years post-transduction *(6)* in humans. However, to date, there have been no successful attempts at treating human monogenic kidney disease. AAV has been used to transduce the rodent kidney *(7, 8)*, mostly through transduction of tubular epithelial cells *(9–13)*,with occasional observations of glomerular and podocyte transduction *(9, 10, 12–15)*. AAV Anc80, a synthetic capsid, has also been shown to transduce kidney mesenchymal cells effectively *(16)*. Dosing in these studies ranged from $5x10^{10}$ to $8.4x10^{12}$ vector genomes (vg) per mouse, where the highest dose administered was of AAV 2/9 to a pregnant mouse and both she and her offspring showed expression in podocytes *(10)*. In theory the podocyte is an ideal target for AAV transduction, because it has cell-specific promoters and it is terminally differentiated, meaning that long-term gene expression is plausible.

Idiopathic nephrotic syndrome is a heterogeneous disease resulting in marked proteinuria, hypoalbuminemia and edema. Central to its pathogenesis is podocyte dysfunction and resultant disruption of the glomerular filtration barrier (GFB) *(17)*. About 10% of children with nephrotic syndrome have a steroid-resistant form of the disease, which has a high morbidity. Many of these children progress to end-stage renal disease, requiring renal replacement therapy or transplantation in childhood *(18)*. About one third of cases of childhood steroid-resistant nephrotic syndrome (SRNS) are genetic *(18–20)*. Of these, the

most common mutations in childhood are in *NPHS2,* encoding podocin, accounting for 10-30% of sporadic genetic cases *(21)*. Currently, there is no effective targeted treatment for the majority of children with genetic nephrotic syndrome *(22–24)*. As such, there is an unmet need for medical therapies for these children.

Podocin is a 42kDa hairpin-like membrane-associated podocyte-specific protein that is a key component of the protein complex at the slit diaphragm, the cell-cell junction between adjacent podocyte foot processes *(25)*. It localises to lipid rafts at the plasma membrane *(26)* and interacts with other important slit diaphragm proteins including nephrin, CD2AP (CD2-Associated Protein) and TRPC6 (Transient Receptor Potential Cation Channel, subfamily C, member 6) *(27)*. It is essential in the maintenance of the slit diaphragm and consequently the integrity of the GFB. There are 126 pathogenic mutations reported in this protein to date *(21)*, but the most common mutation is R138Q, which causes mislocalization of podocin to the endoplasmic reticulum *(28)*. Both the inducible podocin knock-out and podocin mutation knock-in mouse models recapitulate the human disease well, developing proteinuria within eight to fourteen days of induction *(29, 30)*. The inducible podocin knock-out model has loxP sites flanking exon 2 of *NPHS2*, and the doxycycline-induced expression of podocyte specific Cre-recombinase results in deletion of this exon, resulting in a podocin knock-out *(29)*. The inducible podocin knock-in model has the floxed exon 2 of *NPHS2* on one allele and R140Q *NPHS2* (analogous to the missense mutation R138Q podocin in humans) on the other allele *(30)*. Doxycycline induction in this mouse results in excision of the wild-type allele, and therefore the expression of only R140Q podocin, which is retained in the endoplasmic reticulum. Both mouse models demonstrate progression to renal failure, hyperlipidaemia, hypertension and reduced survival *(29)*. The histological findings include early foot process effacement on electron microscopy with little change on light microscopy, and eventual progression to focal segmental glomerulosclerosis (FSGS) *(29)*.

Gene therapy for SRNS would need to transduce the podocyte effectively, express specifically in the podocyte and demonstrate long-term expression. Here, we aimed to identify an AAV serotype that transduces the podocyte effectively, test previously described podocyte-specific promoters within the AAV system, and test AAV-expressing wild type podocin in genetic models of nephrotic syndrome.

RESULTS

AAV-LK03 serotype with a constitutive cytomegalovirus (CMV) promoter or a minimal human nephrin promoter (hNPHS1) transduces human podocytes but not mouse podocytes efficiently in vitro

First, we compared the constitutive CMV promoter versus a minimal human nephrin (podocyte-specific) promoter, hNPHS1 *(31)*, using a green fluorescent protein (GFP) reporter as the readout. AAV-LK03 CMV GFP and AAV-LK03 hNPHS1 GFP WPRE (Fig. 1A) were used to transduce human podocytes (Pod), human glomerular endothelial cells (GEnC) and human proximal tubular epithelial cells (PTEC) at a multiplicity of infection (MOI) of $5x10^5$. WPRE is the Woodchuck Hepatitis Virus Posttranscriptional Regulatory Element, which can increase transgene expression *(32–35)*. Immunofluorescence (Fig. 1, B to D) and Western blot (Fig. 1E) demonstrated GFP expression in all three cell types for AAV-LK03 CMV GFP with only human podocytes showing GFP expression for AAV-LK03 hNPHS1 GFP WPRE. Flow cytometry (n=3) showed that AAV-LK03 CMV GFP had highly efficient expression in human podocytes (% GFP expression=98.83±0.84), AAV-LK03 hNPHS1 GFP WPRE had good expression (% GFP expression=71.3±3.39), and untransduced cells had poor expression (% GFP expression=0.89±0.36) (Fig. 1F). Although the proportion of cells positive for GFP expression was fairly high in human podocytes transduced with AAV-LK03 hNPHS1 GFP WPRE, the cells had a lower median fluorescence intensity than those transduced with AAV-LK03 CMV GFP (Fig. 1G). AAV-LK03 CMV GFP also showed efficient transduction of human proximal tubular epithelial cells (% GFP expression=96.81±0.86), but minimal expression was seen using AAV-LK03 hNPHS1 GFP WPRE (% GFP expression=3.96±1.56) (Fig. 1F). AAV-LK03 CMV GFP showed markedly lower transduction in human glomerular endothelial cells (% GFP expression=7.35±0.19). AAV-LK03 hNPHS1 GFP WPRE showed

minimal transduction in human glomerular endothelial cells (% GFP expression=0.59±0.10), similar to untransduced human glomerular endothelial cells (% GFP expression=0.23±0.02) (Fig. 1F).

Because AAV 2/9 has demonstrated good transduction in kidney cells in vivo in rodent kidneys *(9, 10)*, we tested the expression of AAV 2/9 CMV GFP on human kidney cell lines. AAV 2/9 CMV GFP showed low transduction efficiency in both human podocytes (% GFP expression= 13.9±1.98) and human glomerular endothelial cells (% GFP expression=21.99±4.35) (Fig. 1F). WPRE was included in all constructs used for in vivo work, because omission of this element resulted in a decrease in gene expression in human podocytes in vitro, both on flow cytometry (% GFP expression AAV-LK03 hNPHS1 GFP WPRE= 71.30±3.39 versus AAV-LK03 hNPHS1 GFP=45.93±4.34, n=3) and western blot densitometry (Fig. 1, F to H).

Next, we tested AAV 2/9 and AAV-LK03 on mouse podocytes in vitro. Mouse podocytes demonstrated a different transduction profile from human podocytes. AAV 2/9 CMV GFP on mouse podocytes (% GFP expression=16.26±3.89) showed that nearly three times the number of cells had GFP expression compared to AAV-LK03 CMV GFP (% GFP expression=6.024±1.31) (Fig. 1I).

AAV-LK03-expressing human podocin demonstrates functional rescue in the mutant podocin R138Q human podocyte cell line

Next, we introduced wild-type human podocin into podocin-mutant human podocytes. Podocin normally moves through the endoplasmic reticulum to reach the plasma membrane, where it is associated with other membrane proteins like nephrin *(26, 28)*. In the R138Q podocin mutant, podocin is retained in the endoplasmic reticulum, and does not reach the

plasma membrane *(28)*. Previously, mutant podocin homozygous R138Q podocyte cells were derived from a patient nephrectomy specimen and conditionally immortalised using the temperature sensitive SV40 T antigen *(36)*. AAV-LK03 hNPHS1 hpod (Fig. 2A) transduced both conditionally immortalised R138Q and wild type (WT) human podocytes and expressed Haemagglutinin (HA)-tagged podocin (Figure 2, B to G). HA-tagged podocin was seen at the plasma membrane on confocal microscopy (Fig. 2, B, C and E, white arrow) and colocalised with caveolin-1, a lipid raft protein, as seen on TIRF (Total Internal Reflection Fluorescence) microscopy (Fig. 2,D and F). Untransduced R138Q human podocytes did not show any podocin expression at the plasma membrane (Fig. 2, B and F). Wild type human podocytes showed a small amount of podocin expression at the plasma membrane, and this was increased in transduced WT human podocytes (Fig. 2E, white arrow showing plasma membrane expression). HA-tagged podocin colocalized with calnexin, an endoplasmic reticulum marker, but also showed expression at the plasma membrane (Fig. 2, C and F white arrow to show plasma membrane expression). This is consistent with podocin processing and trafficking, via the endoplasmic reticulum to the plasma membrane.

Podocytes have demonstrated alterations in adhesion in diseased states. R138Q human podocytes showed reduced adhesion compared to wild type human podocytes transduced with control virus. Transduction with AAV-LK03 hNPHS1 hpod resulted in a partial rescue of adhesion of R138Q human podocytes, demonstrating a partial degree of functional rescue (Fig. 2H).

Inducible podocin knock-out mice demonstrate features of nephrotic syndrome

The Pod-rtTA TetO-Cre $NPHS2^{fl/fl}$ mice (inducible podocin knockout nephrotic mice) were tested to check that they developed the expected phenotype as described in *(29)*.

Controls were littermates with the full genotype who received 5% sucrose as drinking water (no doxycycline controls), and littermates who were either lacking the Pod-rtTA or TetO-Cre genes (incomplete genotype controls) who were given doxycycline water. Mice were culled when they showed severe signs of illness (Bristol Generic Welfare Score Sheet, and in discussion with Named Animal Care & Welfare Officer). Mice who were otherwise clinically well were culled at 25 weeks post initiation of doxycycline.

The effect of the correct genotype with administration of doxycycline on urinary albumin creatinine ratio (ACR) was significant (Fig. 3A, two-way ANOVA, $P<0.0001$, n=4/group). The increase in urinary ACR is significant by day 21 (Fig. 3A, Pod-rtTA TetO Cre NPHS2$^{fl/fl}$ + doxycycline= 10,759.7±2388.5mg/mmol, Pod-rtTA TetO Cre NPHS2$^{fl/fl}$ – doxycycline= 3.4±0.9mg/mmol, and incomplete genotype + doxycycline= 4.6±1.1mg/mmol, $P<0.05$, n=4/group). Mice in the two control groups continued to have low urinary ACRs until they were culled 25 weeks post induction with doxycycline (Pod-rtTA TetO Cre NPHS2$^{fl/fl}$ – doxycycline= 27.0±16.0mg/mmol, incomplete genotype + doxycycline= 13.8±7.6mg/mmol).

Conditional podocin knockout mice had a reduced survival, with a median survival of 66 days (range 33 to 126 days). Mice from the incomplete genotype and no doxycycline control groups survived until they were culled at the end point of 25 weeks post doxycycline. This reduction in survival was significant (Fig. 3B, Log-rank (Mantel-Cox) test, $P=0.0012$, n=4/group).

Pod-rtTA TetO-Cre NPHS2$^{fl/fl}$ mice given doxycycline showed a raised plasma creatinine at 10 weeks post induction (Fig. 3C, one-way ANOVA, $P=0.035$, n=2-4/group). These mice had a significantly raised creatinine (Fig. 3D, one-way ANOVA, $P=0.031$, n=2-4/group), urea (Fig. 3E, one-way ANOVA, $P<0.001$, n=2-4/group) and cholesterol (Fig. 3F, one-way ANOVA, $P=0.0064$, n=2-4/group) at death.

Kidney histology of Pod-rtTA TetO-Cre NPHS2$^{fl/fl}$ mice given doxycycline showed glomeruli that were diffusely and globally sclerosed. Tubular atrophy and dilatation, along with interstitial fibrosis was also observed. Control mice showed normal kidney histology (Fig. 3G).

Intravenous injection of AAV serotype 2/9 demonstrates transduction of the podocyte

Next, we tested efficiency of transduction of HA-tagged podocin in vivo, comparing either a human nephrin or mouse nephrin promoter construct. Here, we switched to using AAV 2/9 because our in vitro data on mouse podocytes above (Fig. 1I) suggested superior transduction efficiency when comparing AAV 2/9 to AAV-LK03, and the published literature has also demonstrated expression in the glomerulus using AAV 2/9 *(9, 10, 12, 13)*. At 8 weeks of age, Pod-rtTA TetO-Cre NPHS2$^{fl/fl}$ mice were administered 1.5 x 10^{12} vg (about 6 x 10^{13}vg/kg) via tail vein of either AAV 2/9 hNPHS1.mpod or AAV2/9 mNPHS1.mpod or saline (Fig. 4, A and B). Both minimal mouse and human nephrin promoters were tested in this experiment, because it was uncertain if both promoters were equally efficacious in mice. Eight weeks later, AAV ITRs (inverted terminal repeat) were detected in the kidney cortex of mice injected with AAV (AAV 2/9 hNPHS1.mpod=39,067±13,285 copies ssDNA per 50ng DNA, AAV 2/9 mNPHS1mpod=76,533.33±32047 copies ssDNA per 50ng DNA, *n*=5-6/group) (Fig. 4C). Mice injected with AAV vector demonstrated increased podocin mRNA and increased HA-tagged podocin mRNA (Fig. 4, D and E). HA-tagged podocin was shown to co-localize with the podocyte markers nephrin and podocin (Fig. 4F). Pod-rtTA TetO-Cre NPHS2$^{fl/fl}$ mice that were administered saline showed a loss of podocin and a diffuse pattern of nephrin staining (Fig. 4G). This is in stark contrast to the membrane localized pattern seen for both proteins in AAV-treated Pod-rtTA TetO-Cre NPHS2$^{fl/fl}$ mice (Fig. 4F). Transduction efficiency calculated by quantification of HA-tag immunofluorescence (*n*=3) was

0.109±0.053 for AAV 2/9 hNPHS1.mpod and 0.115±0.029 for AAV 2/9 mNPHS1.mpod (Fig. 4H).

AAV2/9 expressing wild type podocin administered prior to disease induction partially reduces albuminuria and improves the phenotype in inducible podocin-knockout nephrotic mice

To maximise the effect of the AAV gene therapy, we initially used a prophylactic approach where AAV 2/9-expressing wild type podocin was administered systemically before disease induction with doxycycline. Doxycycline induction of podocin gene knock out commenced 10-14 days after AAV tail vein injection in Pod-rtTA TetO-Cre $NPHS2^{fl/fl}$ mice (Fig. 4B). Groups treated with AAV 2/9 hNPHS1.mpod or AAV 2/9 mNPHS1.mpod showed a significant reduction in albuminuria at days 14, 28 and 42 after onset of doxycycline induction (Fig. 5, A and B). At 14 days after induction, the urinary albumin: creatinine ratio (ACR) was significantly higher in the saline group than either of the vector treated groups (Fig. 5A, saline = 3,770.1±1337.6 mg/mmol, AAV 2/9 hNPHS1.mpod = 758.1±488.1 mg/mmol, AAV 2/9 mNPHS1.mpod = 59.8±28.0 mg/mmol, one-way ANOVA P=0.0091, Dunnett's multiple comparisons, AAV 2/9 hNPHS1.mpod vs saline P=0.0297, AAV 2/9 mNPHS1.mpod vs saline P=0.0075, n=9 per group). There was a significant reduction in urinary ACR in the vector-treated groups at day 28 (Fig. 5A, saline = 10,198±3,189.5 mg/mmol, AAV 2/9 hNPHS1.mpod = 3,083.0±932.8 mg/mmol, AAV 2/9 mNPHS1.mpod = 2,195.1±778.9 mg/mmol, one-way ANOVA P=0.0158, Dunnett's multiple comparisons, AAV 2/9 hNPHS1.mpod vs saline P=0.0323, AAV 2/9 mNPHS1.mpod vs saline P=0.0158, n=9 per group) and day 42 (Fig. 5A, saline = 13,488.8±3,877.3 mg/mmol, AAV 2/9 hNPHS1.mpod = 3,266.8±1,212.2 mg/mmol, AAV 2/9 mNPHS1.mpod =3,553.3±1,477.87

mg/mmol, one-way ANOVA *P*=0.0113, Dunnett's multiple comparisons, AAV 2/9 hNPHS1.mpod vs saline *P*=0.0149, AAV 2/9 mNPHS1.mpod vs saline *P*=0.0179, n=9 per group). In the vector-treated groups, 2 of 9 mice in AAV 2/9 hNPHS1.mpod group and 1 of 9 mice in AAV 2/9 mNPHS1.mpod group had urinary ACRs of less than 30mg/mmol at day 42.

Although the mice in vector-treated groups showed an improvement, there was a large degree of variation within the groups which we hypothesised might be attributable to amount of vector that reached the kidney after a systemic injection. Consistent with this, the amount of viral DNA detected in kidney cortex showed a weak though significant inverse correlation with the degree of albuminuria at days 28 (Fig. 5C, Spearman r=-0.4965, *P*=0.0306) and 42 (Fig. 5D, Spearman r= -0.4596, *P*=0.0477).

Vector-treated mice showed an improvement in plasma markers of kidney disease. There was a significant difference between saline and vector-treated mice for plasma creatinine (Fig. 5E, saline=43.0±7.2µmol/L, AAV 2/9 hNPHS1.mpod=25.3±6.4µmol/L, AAV 2/9 mNPHS1.mpod = 18.6±4.4µmol/L, one-way ANOVA *P*=0.0462, Dunnett's multiple comparison, AAV 2/9 mNPHS1 mpod versus saline *P*<0.05, *n*=4-5/group), and urea concentrations (Fig. 5F, saline=66.4±27.8mmol/L, AAV 2/9 hNPHS1.mpod=14.0±2.5mmol/L, AAV 2/9 mNPHS1.mpod=11.6±1.6mmol/L, one-way ANOVA *P*=0.041, Dunnett's multiple comparisons, AAV 2/9 hNPHS1.mpod vs saline *P*<0.05, AAV 2/9 mNPHS1.mpod vs saline *P*<0.05, *n*=4-5/group). There was a significant reduction in cholesterol concentrations in vector-treated mice (Fig. 5G, saline=13.2±2.8mmol/L, AAV 2/9 hNPHS1.mpod=4.4±1.8mmol/L, AAV 2/9 mNPHS1.mpod=4.86±0.76 mmol/L, one-way ANOVA *P*=0.0192, Dunnett's multiple comparisons, AAV 2/9 hNPHS1.mpod vs saline p<0.05, AAV 2/9 mNPHS1.mpod vs saline

P<0.05, n=3-4/group). There was no significant change in albumin in vector-treated mice (Fig. 5H, saline=11.2±3.9 g/L, AAV 2/9 hNPHS1.mpod 18.6±4.0g/L, AAV 2/9 mNPHS1.mpod=17.1±3.6g/L, one-way ANOVA *p*=0.4097, *n*=4-5).

Saline-treated mice demonstrated histological features of glomerulosclerosis (Fig. 6A, black arrow) by 6 weeks, some of which was diffuse and global. These mice also showed tubular atrophy (Fig. 6A, black arrowhead) and interstitial fibrosis. AAV-treated mice demonstrated a range of histological findings, from completely normal glomeruli to mesangial hypercellularity to a few glomeruli with glomerular sclerosis (Fig. 6, A to D). Blinded quantification of the histological sections showed a statistically significantly lower proportion of sclerosed glomeruli in AAV-treated mice compared to saline-treated mice (Fig. 6B, two-way ANOVA, *P*=0.0004). Dunnett's multiple comparisons showed significant reduction in global sclerosis (AAV 2/9 hNPHS1.mpod vs saline *P*=0.0012, AAV 2/9 mNPHS1.mpod vs saline *P*=0.0188), but no significant difference in segmental sclerosis (AAV 2/9 hNPHS1.mpod vs saline *P*=0.0513, AAV 2/9 mNPHS1.mpod vs saline *P*=0.0982), *n*=5-6/group), and there was no significant difference in the extent of mesangial hypercellularity (Fig. 6C, one-way ANOVA *P*=0.8825, *P*=5-6/group). Overall, there was no significant difference in interstitial fibrosis (Fig. 6D, one-way ANOVA *P*=0.0521, *n*=5-6/group), but there was a significant reduction in interstitial fibrosis when comparing AAV 2/9 hNPHS1.mpod vs saline (Fig. 6D, Dunnett's multiple comparison *P*=0.0327). On electron micrographs, saline-treated Pod-rtTA TetO-Cre NPHS2$^{fl/fl}$ tended to show podocyte loss (Fig. 6E) or extensive foot process effacement. The AAV-treated mice again showed a range of findings, with some areas showing complete foot process effacement, whereas other areas showed evenly spaced foot processes (Fig. 6E). Overall, there was no significant change in number of foot processes per micron GBM (Glomerular Basement Membrane)

(Fig. 6F, one-way ANOVA P=0.0503, n=3/group), however there was a significant increase when comparing AAV 2/9 hNPHS1.mpod vs saline (Fig. 6F, Dunnett's multiple comparison P=0.0385).

AAV-treated mice also showed prolonged survival (n=3-4/group), with a median survival of 192 days (range 74 to 365 days, mice were culled at 365 days) in AAV 2/9 hNPHS1.mpod treated mice and median survival of 192 days (range 131 to 365 days, mice were culled at 365 days) in AAV 2/9 mNPHS1.mpod treated mice, compared to a median survival of 75.5 days (range 38 to 111 days) in the saline group (Log-rank (Mantel-Cox) test, P=0.0276). (Fig. 6G)

AAV 2/9- expressing wild type podocin administered after onset of proteinuria partially reduces albuminuria and improves the phenotype in inducible podocin knock-in nephrotic mice

Next, we tested AAV2/9 hNPHS1.mpod in inducible R140Q mutant podocin knock-in mice (Pod-rtTA TetO-Cre NPHS2$^{fl/R140Q}$) *(30)*. In this hemizygous conditional knock-in model, when doxycycline is administered, *NPHS2* on one allele is knocked out while the other *NPHS2* allele with the R140Q mutation is expressed. R140Q podocin is the mouse analog of R138Q podocin in humans, which is the most common podocin mutation found in childhood nephrotic syndrome *(21, 37)*. Here, two weeks after initiation of doxycycline in Pod-rtTA TetO-Cre NPHS2$^{fl/R140Q}$ mice, urine was collected. Proteinuria was confirmed by dipstick analysis of 3+ or more. Mice were then administered 1.5 x 10^{12} vg (about 6 x 10^{13}vg/kg) of AAV 2/9 hNPHS1.mpod or saline via tail vein injection. (Fig. 7A) We did not test AAV 2/9 mNPHS1.mpod in this model, because we had demonstrated equivalence to

AAV 2/9 hNPHS1.mpod in the previous experiment, and the minimal human nephrin promoter would be more relevant for translation.

Mice were treated with AAV hNPHS1.mpod or saline at day 14, and a significant reduction in urinary albumin: creatinine ratio was seen in treated mice by day 42 [Fig. 7B, saline=2,951±1,060 mg/mmol (n=5), AAV 2/9 hNPHS1.mpod= 943.5±335.3 mg/mmol (n=9), Unpaired *t*-test, *P*=0.0436) and day 56 after initiation of doxycycline (Fig. 7B, saline=8,361±4,281 mg/mmol (*n*=5), AAV 2/9 hNPHS1.mpod=514.1±177.7 mg/mmol (*n*=9), Unpaired *t*-test, *P*=0.0261]. Mice in the two groups showed no differences in plasma creatinine (Fig. 7C, saline=18.8±1.9µmol/L, AAV 2/9 hNPHS1.mpod=14.4±2.4µmol/L, Unpaired *t*-test *P*=0.182) and cholesterol concentrations (Fig. 7D, saline=3.2±0.08mmol/L, AAV 2/9 hNPHS1.mpod=3.6±0.37mmol/L, Unpaired *t*-test *P*=0.152). Treated mice had a significantly higher serum albumin concentration (Fig. 7E, saline=26.7±1.0g/L, AAV 2/9 hNPHS1.mpod=30.8±1.0g/L, Unpaired *t*-test *P*=0.0119).

The histology (Fig. 7F) at 56 days after doxycycline induction demonstrated marked glomerulosclerosis (black arrow) and interstitial fibrosis (black arrowhead) in saline-treated mice, whereas AAV-treated mice showed less sclerosed glomeruli, with mesangial hypercellularity in some glomeruli. On electron microscopy (Fig. 7G), saline-treated mice showed widespread foot process effacement (black arrow) while AAV-treated mice showed areas of normal foot process morphology (white arrow) alongside areas with foot process effacement (black arrow).

Lastly, HA-tagged podocin was shown to co-localise with podocyte marker nephrin (Fig. 8A, top panels). Pod-rtTA TetO-Cre NPHS2$^{fl/R140Q}$ mice that were administered saline showed a loss of nephrin staining (Fig. 8A, bottom panels).

AAV 2/9 expressing wild type podocin under the human minimal nephrin promoter demonstrates extra-renal expression in inducible podocin knock-in nephrotic mice

We tested for specificity of the minimal human nephrin promoter in our inducible podocin knock-in mice. We found that the expression of the minimal human nephrin promoter is not restricted to the glomerulus. RNAScope, an *in situ* hybridization assay, was used to detect AAV transcripts by using an anti-sense probe for WPRE. This demonstrated the presence of transcripts in the kidney glomerulus, as well as in the liver and spleen, though not in pancreas (Fig. 8B). qPCR confirmed these findings and demonstrated a mean fold change of 10 or above in kidney, liver and spleen (Fig. 8C).

DISCUSSION

The podocyte, being a terminally differentiated cell, is in theory an excellent target for gene therapy, as gene transfer can be lifelong. Our study demonstrates that potential, as important proof of concept for a translational gene therapy program.

Here we tested AAV-LK03 on kidney cells, showing high transduction in human podocytes and proximal tubular cells. Lisowski et al demonstrated that AAV-LK03 transduced human hepatocytes highly efficiently, but transduced mouse hepatocytes poorly *(38)*. One factor determining the tropism of each serotype is the use of different cell surface receptors and coreceptors for binding. AAV-LK03 is closely related to AAV3 *(39)*, which uses heparin sulphate proteoglycan as its main receptor for cellular entry, with human hepatocyte growth factor receptor (c-Met) acting as a coreceptor *(40)*. Transduction of human hepatocytes by AAV-LK03 in vitro was competitively inhibited by human hepatocyte growth factor *(38)*. C-Met is expressed in many epithelial cells, including human podocytes *(41)* and proximal tubular cells, which partially explains the strong transduction profile in our human kidney epithelial cells.

We showed that expression of wild type podocin in the R138Q mutant podocytes results in partial rescue of adhesion. Podocyte cytoskeletal changes are well established as correlates of functional loss of barrier integrity *(42)*, for example, several single gene mutations in *TRPC6*, *MAGI2*, *DLC1*, *CDK20* directly affect cytoskeletal pathways and demonstrably alter podocyte motility *(43, 44)* . Loss of podocyte adhesion leads to podocyte loss *(42)*, and it has been previously demonstrated that the degree of podocyte loss correlates to the degree of proteinuria and glomerulosclerosis in rat models *(45)*.

Using AAV-LK03 has implications for clinical use: effective transduction of human podocytes might enable a reduction in effective dose in humans. A recent UK study has shown a low anti-AAV-LK03 neutralizing antibody seroprevalence of 23% *(46)*, which

makes this particular serotype a promising candidate for translational studies. We showed that AAV-LK03 was a poor transducer of mouse podocytes in vitro and hence moved to AAV 2/9 for the in vivo mouse work.

We successfully targeted the murine podocyte with AAV 2/9 in both the inducible podocin knock-out and knock-in mouse models, with improved albuminuria in vector-treated mice. To maximize effect, we initially chose a prophylactic approach in the inducible podocin knock-out model. Next, we administered the AAV 2/9 vector after onset of proteinuria in inducible podocin knock-in mice, mimicking the clinical scenario of therapeutic delivery after onset of disease in a mouse model analogous to the most common human *NPHS2* mutation. It will be important to test whether gene therapy administered later in the disease course can demonstrate the same rescue, because there is no current evidence that guides us in determining when the kidney pathology becomes irreversible. Convention is that the nephron is fully differentiated before birth in humans and in the perinatal period in mice *(47)*, but there is some evidence that glomerular parietal epithelial cells might be able to differentiate into podocytes and have regenerative potential after birth *(48, 49)*.

We note that there is variability in the degree of albuminuria in both our treated and untreated mice. The variability could be due the amount of viral transduction in the kidney or the mixed background used in the inducible podocin knock-out model, where other genes may influence the kidney's ability to compensate for the loss of podocin. This is certainly the case in humans, where carrying 2 *APOL1* risk alleles is correlated with earlier onset of FSGS and earlier progression to end stage renal disease *(50)*.

The glomerular filtration barrier does not normally allow large proteins to pass through. AAV vectors have to pass through the glomerular endothelial cell fenestrations and cross the glomerular basement membrane to reach the podocyte. AAV is small enough to pass through the glomerular endothelial cell fenestrations (60-70nm) *(51)*. AAV has also

been found in urine in non-human primates and mice *(52, 53)*, suggesting that AAV is able to pass through despite a potential physical barrier at the podocyte slit diaphragm. One potential way through the podocyte barrier might be via endocytosis, followed by exocytosis. In our disease models, it is likely that AAV might traverse the damaged glomerular filtration barrier more easily, although we have not looked at this specifically in our study.

Here, we chose a systemic injection which would result in predominantly liver transduction *(7)*. We demonstrated a relatively low podocyte transduction efficiency in vivo of about 10%, as detected by immunofluorescence against the HA-tag. However, our assay might be insensitive in truly detecting viral transduction, because the HA-tag at the C terminus might be removed during post-translational processing. Alternatively, it is possible that a small number of podocytes were transduced by the AAV vector, which was sufficient to reduce albuminuria. We feel that the assay likely underestimates podocyte transduction, because more sensitive methods of detecting transduction have shown a good amount of glomerular transduction using AAV9 using lower doses, although immunostaining was not carried out to demonstrate the cell type transduced *(15)*. The amount of AAV DNA found in the kidney cortex in this study is several fold lower than that found in the liver by other groups *(7, 54)*. Improved transduction of kidney cortex by renal vein injection of AAV9 to the murine kidney has previously been shown *(9)*. Future steps to making AAV vectors for the kidney translational would be to test the effect of different delivery routes in large animal models, including direct renal artery injection, on specificity and transduction efficiency.

We attempted to direct expression to the podocyte by using the minimal human and mouse nephrin promoters. These have previously been shown to be mostly podocyte specific *(31, 55)*. In this study, immunofluorescence suggested that expression co-localized with podocyte markers, although the glomerulus is well known to be densely packed with several cell types. Our in vitro work showed that inclusion of the minimal nephrin promoter led to

expression of the transgene in podocytes, and not in glomerular endothelial cells, which makes it likely that the glomerular expression seen is in podocytes. When the minimal human nephrin promoter was used with AAV vectors in the conditional podocin knock-in mouse, there were high amounts of transcript in the liver and spleen. One previous study injected 1 x 10^{12} vector genomes per mouse of AAV 2/9 hNPHS1 GFP in wild type mice and demonstrated some expression in the liver and spleen, but at lower amounts than that seen in the kidney *(10)*. We used a higher AAV dose in nephrotic mice. These mice lose large amounts of albumin and IgG, and thus will have transcriptionally active livers and lymphocytes. Although integration was low for AAV (estimated 0.1%) *(56)*, the transcriptionally active liver and spleen in combination with the high dose administered might have resulted in integration of our vector and expression of transcript in the liver and spleen. A second explanation could be that this minimal human nephrin promoter is not sufficiently specific, and we are currently testing different promoter sequences to improve specificity.

The dose used in the mouse studies here was high at 1.5 x 10^{12} vector genomes per mouse, which could trigger unwanted immune responses. We plan to test whether lower doses are equally efficacious. In parallel, it will be important to engineer AAV capsids that preferentially transduce the podocytes without triggering unwanted immune responses, potentially facilitating a lower vector dose requirement and reducing off-target expression *(57)*.

There are some limitations to our study. As discussed above, there was variability in the amount of proteinuria seen in the mouse model despite our efforts to ensure consistency in mouse background. However, both the in vitro work and in vivo work were carried out on well-validated pre-clinical models, and both demonstrate partial rescue of adhesion and proteinuria, suggesting potential to translate these findings to the clinic. It is difficult to

predict the functional effect of off-target extra-renal expression of podocin, and this would require either longer term monitoring of effects, or improvements in targeting to the podocyte either by promoter and capsid optimization or by a directed renal injection. We did not monitor immune responses or toxicity in these studies, which will be required before translation to ensure that doses are safe and tolerable. Switching serotypes from AAV 2/9 in mice to AAV-LK03 to translate the gene therapy will be another hurdle and will require further AAV-LK03 studies in large animals to demonstrate efficacy, safety, and tolerability, and to calculate an appropriate dose for translation.

In conclusion, we demonstrated AAV transduction of podocytes, and provided evidence that this rescues the nephrotic phenotype in both the inducible podocin knock-out and knock-in mouse models. We also showed that the synthetic capsid, AAV-LK03, demonstrates efficient transduction of human podocytes. Although there are still many challenges to be overcome before this work can be translated to humans, including refining the cell-specific targeting of AAV to the podocyte, this work demonstrates a first step towards AAV gene therapy targeting monogenic diseases of the podocyte.

MATERIALS AND METHODS

Study design

This study investigated using AAV to target the podocyte for the treatment of genetic nephrotic syndrome due to *NPHS2* mutation. AAV transduction using both a constitutive and podocyte-specific promoter was evaluated in vitro on wild type conditionally immortalized human podocytes, human glomerular endothelial cells, human proximal tubular cells and mouse podocytes. AAV expressing wild type podocin was tested on conditionally immortalized human podocyte carrying a naturally occurring *NPHS2* mutation (commonest

cause of childhood genetic nephrotic syndrome). Each experiment was performed in at least biological triplicate.

All animal experiments and procedures were approved by the UK Home Office in accordance with the Animals (Scientific Procedures) Act 1986, and the Guide for the Care and Use of Laboratory Animals was followed during experiments. We tested high dose AAV expressing podocin against a saline control in two mouse models, the inducible podocin knockout and knockin models. Each animal was considered an experimental unit, and the experiment was run in small batches of between 2-6 animals depending on the correct genotypes from breeding trios. In vivo experimental batches were independently repeated by at least two different researchers. Littermate controls were used as much as possible. However, a small number of non-littermate controls were used due to the complexity of the breeding scheme, with small numbers of mice within each litter with the desired genotype. Mice were assigned randomly to each experimental group, but confounders were not specifically controlled for. The primary outcome was urinary albumin:creatinine ratio, which was tested every two weeks. We also collected blood and tissue at the end of the experiments. Tissue was processed so that we generated data for a range of results including DNA, RNA, histology, RNAScope and immunofluorescence. Animals were excluded from a specific analysis if there was insufficient urine, tissue or blood sample for that analysis. Histological analyses of the mice were blinded, but otherwise researchers were not blinded. There was no a priori sample size calculation as there was no pilot data for this calculation. This in vivo study design has been reported using the ARRIVE guidelines 2.0.

Vector production

We cloned pAV.CMV.GFP.WPRE.bGH, pAV.hNPHS1.GFP.WPRE.bGH, pAV.hNPHS1.GFP.bGH, pAV.hNPHS1.mpodHA.WPRE.bGH, pAV.mNPHS1.mpodHA.WPRE.bGH, pAV.hNPHS1.hpodHA.WPRE.bGH and pAV.CMV.hpodHA.WPRE.bGH (Fig. 1A, 2A, 4A) in our laboratory from a pAV CMV GIL (CMV eGFP L22Y pUC-AV2) construct (Cloning strategy is described in the supplementary materials and methods, fig. S1, Tables S1to S3). The minimal human nephrin promoter (hNPHS1) was a kind gift from S. Quaggin, Northwestern University. Constructs containing either human or mouse podocin were HA-tagged at the C terminus. Human embryonic kidney 293T cells (cultured in DMEM (Dulbecco's Modified Eagle Medium) with 1mM pyruvate, 25mM glucose, 3.97mM L-glutamine, 10% fetal bovine serum (FBS) and 1% penicillin/streptomycin) were transfected with a capsid plasmid (pAAV9 from Penn Vector Core, pAAV-LK03 was the kind gift of M. Kay, Stanford University), a helper plasmid with adenoviral genes (pHGTI-Adeno1, kind gift of R. Mulligan, Harvard University) and the transgene plasmid using polyethyleneimine 0.1%. Media was changed to serum free DMEM 8 to 24 hours post-transfection. Cells and supernatant were harvested 72 hours after transfection. Cells underwent five freeze-thaw cycles, and the supernatant underwent PEG (Polyethylene glycol) precipitation (8% PEG 0.5N NaCl). These were combined and incubated with 0.25% sodium deoxycholic acid and 70units/ml Benzonase for 30 minutes at 37°C. The vector was purified by iodixanol gradient ultracentrifugation *(58)* using a Type70.1 Ti rotor, and subsequently concentrated in PBS. Vectors were titrated by alkaline gel electrophoresis and qPCR using the standard curve method using the following primers: ITR F GGAACCCCTAGTGATGGAGTT, ITR R CGGCCTCAGTGAGCGA, ITR probe FAM-5'-CACTCCCTCTCTGCGCGCTCG-3'-TAMRA.

Animals

Inducible podocin knockout mice were developed by crossing NPHS2$^{flox/flox}$ mice *(29)* with NPHS2-rtTA/ Tet-On Cre mice (The Jackson Laboratorystrains 008202 and 006234) *(59)* to generate NPHS2-rtTA/ Tet-On Cre/ NPHS2$^{flox/flox}$ mice(Pod-rtTA TetO-Cre NPHS2$^{fl/fl}$). These mice were given oral doxycycline (2mg/ml in 5% sucrose for 3 weeks) from 5 weeks of age to delete podocin, urine was collected weekly, and tissue and blood was collected when culled. Mice were on a predominantly 129/Sv background, with contributions from C57Bl/6 and FVB, and mice from both sexes were used. Next, mice were administered AAV or saline via tail vein injection at 8 weeks of age (Fig. 4B). 12-13 mice were recruited to each experimental group. 10 to 14 days later, mice were provided with drinking water supplemented with doxycycline 2mg/ml in 5% sucrose for 3 weeks. Urine was collected every two weeks. Six mice from each group were culled by Schedule 1 methods at 6 weeks after initiation of doxycycline. A cohort of mice was also kept beyond 6 weeks to test for effect on survival. These were culled at day 365 after initiation of doxycycline. There were no a priori inclusion or exclusion criteria for this group of animals.

Inducible podocin knock-in mice were developed by crossing NPHS2$^{R140Q/+}$ *(30, 37)*, NPHS2$^{flox/flox}$ mice *(29)* with NPHS2-rtTA/ Tet-On Cre mice *(59)* to generate NPHS2-rtTA/ Tet-On Cre/ NPHS2$^{flox/R140Q}$ mice (Pod-rtTA TetO-Cre NPHS2$^{fl/R140Q}$). Mice were on a predominantly 129/Sv background, and mice from both sexes were used. At 6-7 weeks of age, mice were provided with drinking water supplemented with doxycycline 2mg/ml in 5% sucrose for 3 weeks. Doxycycline induction resulted in knockout of *NPHS2* on one allele, leaving the R140Q *NPHS2* on the other allele. Two weeks after initiation of doxycycline, urine was tested via urine dipstick and animals with proteinuria of more than 3+ were randomized to receive saline or AAV. Nine to ten mice were recruited to each experimental group. Urine was collected every 2 weeks and mice were culled at 8 weeks after initiation of

doxycycline (Fig. 7A). Only animals with urine albumin: creatinine ratio of more than 150 mg/mmol in the first four weeks were included in the final analysis.

Cell culture

All conditionally immortalized kidney cell lines were generated inhouse and have been previously reported in detail in the referenced papers. Conditionally immortalized human podocytes *(60, 61)* (Pod) and mouse podocytes *(62)* were cultured in RPMI with L-glutamine and NaHCO3 with 10% FBS and 1% penicillin/ streptomycin at a permissive temperature of 33°C. Conditionally immortalized human glomerular endothelial cells *(63)* (GEnC) were cultured in EBM^{TM}-2 Endothelial Cell Growth Basal Medium-2 supplemented with EGM^{TM}-2 Endothelial Cell Growth Medium-2 BulletKit^{TM} (Lonza) at a permissive temperature of 33°C. Both the conditionally immortalized human podocytes and glomerular endothelial cell lines were immortalized with a SV40 temperature-sensitive T Antigen, and further differentiated into the respective cell types when grown at 37 degrees (10-14 days for podocytes and 5 days for endothelial cells) *(60, 61, 63)*. Immortalized proximal tubule epithelial cells *(64)* (PTEC) were cultured in DMEM/F12 supplemented with insulin, transferrin and selenium (5µg/ml), hydrocortisone (0.4 µg/ml),10% FBS and 1% penicillin/ streptomycin.

Cells at a confluence of about 50% were transduced with AAV at a MOI of 5 x 10^5, and switched to 37°C on the same day to differentiate. For GFP expression, cells were used at 5-7 days after transduction to allow comparisons across different cell lines. For podocin expression, cells were used at 10-14 days after transduction when podocytes are maximally differentiated.

Quantitative PCR

DNA was extracted using DNeasy Blood and Tissue Kit (Qiagen) from mouse kidney cortex. AAV DNA was detected using the same primers as above (ITR F, ITR R, ITR probe) for viral titration. RNA was extracted using RNeasy Mini Kit with RNase-Free DNase set (Qiagen). 1µg of RNA was converted to cDNA. The following primers were used for qPCR on cDNA: PodHA F CAGAGCACAAGGGAGCATCA, PodHA R AGCGTAATCTGGAACATCGTATGG, NPHS2 total F TTGATCTCCGTCTCCAGACCTT, NPHS2 total R TCCATGCGGTAGTAGCAGACA, 18S F AGTTGGTGGAGCGATTTGTC and 18S R CGGACATCTAAGGGCATCAC.

RNAScope

RNAScope was carried out on formalin fixed paraffin embedded sections as per the manufacturer's protocol using the WPRE-O4 probe, with an additional step of 0.3M HCl for 30 minutes at room temperature before the hydrogen peroxide step. Briefly, slides were deparaffinized, then exposed to 0.3HCl for 30 minutes to eliminate endogenous alkaline phosphatase activity. Hydrogen peroxide was applied for 10 minutes at room temperature, then sections were boiled in target retrieval solution for 15 minutes (kidney, spleen, pancreas) or 30 minutes (liver). Sections were then incubated with protease plus at 40°C for 30 minutes. The probe was applied for 2 hours at 40°C, then the sections were subject to sequential amplification steps. The last amplification probe was conjugated with alkaline phosphatase, which reacts with Fast Red Chromogen Substrate, resulting in a red punctate signal which can be seen on bright field microscopy.

Immunofluorescence

5µm sections were fixed using 4% PFA and blocked with 3% BSA 0.3% Triton X-100 and 5% of either goat or donkey serum (depending on the species the secondary antibody was raised

in). Primary antibodies were anti-HA High Affinity from rat IgG_1 (Roche,Cat#: 11867423001), Guinea Pig anti-Nephrin (1243-1256) Antibody (Origene,Cat#: BP5030), and Rabbit anti-NPHS2 Antibody (Proteintech, Cat#: 20384-1-AP).

Cells were fixed with either 4% PFA and or ice cold methanol, incubated for 5 minutes with 0.03M glycine, permeabilized with 0.3% Triton then blocked with 3% BSA. Primary antibodies were mouse anti-HA.11 Epitope Tag Antibody (Biolegend, Cat#: 901516), mouse anti-GFP (Roche, Cat#: 11814460001), rabbit anti-Calnexin (Merck Millipore, Cat#: C4731) and rabbit anti-Caveolin 1 (Cell Signaling Technology, Cat#: 3267).

Secondary antibodies were AlexaFluor 488 donkey anti-mouse, AlexaFluor 488 donkey anti-rabbit, AlexaFluor 488 goat-anti guinea pig, AlexaFluor 555 goat anti-rabbit and AlexaFluor 633 goat anti-rat, and AlexaFluor 633 Phalloidin (Invitrogen, Thermo Fisher Scientific). Sections or cells were counterstained with DAPI and mounted with Mowiol. Images were taken on a Leica SPE single channel confocal laser scanning microscope attached to a Leica DMi8 inverted epifluorescence microscope, or Leica SP5-II confocal laser scanning microscope attached to a Leica DMI 6000 inverted epifluorescence microscope, or Leica AM TIRF MC (multi-colour) system attached to a Leica DMI 6000 inverted epifluorescence microscope using LAS (Leica Application Suite) X Software.

Quantification was performed using Fiji *(65)*. A region of interest was drawn around each glomerulus, and integrated density, mean fluorescence and area were calculated for both nephrin and HA immunofluorescence. The mean background fluorescence was calculated for each channel and corrected total cell fluorescence (CTCF) was calculated [CTCF=integrated density-(area of glomerulus x mean background fluorescence)]. Fluorescence of HA was then normalized to nephrin for each glomerulus.

Western blotting

Cells were extracted in SDS lysis buffer. Samples were run on a 12.5% gel and transferred to PVDF membrane. Membranes were blocked in 5% milk in TBST 0.1%. Primary antibodies used were mouse anti-HA.11 Epitope Tag Antibody (Biolegend, Cat#: 901516), mouse anti-GFP (Roche, Cat#: 11814460001)in 3% BSA in TBST 0.1%, or rabbit anti-NPHS2 antibody (Proteintech, Cat#: 20384-1-AP, validated in fig. S1B). Secondary antibodies were anti-rabbit or anti-mouse IgG Peroxidase (Sigma Aldrich) in 3% BSA in TBST 0.1%. Membranes were imaged on Amersham Imager 600.

Flow cytometry

Cells were stained with propidium iodide and only live single cells were included in the analysis. Flow cytometry was carried out on the NovoCyte Flow Cytometer.

Adhesion assay

Podocytes which had been differentiated at 37°C for 10-14days were trypsinized and resuspended at 10^5/ml and allowed to recover for 10 minutes before plating 50µl of cells diluted 1 in 2 with PBS in a 96 well plate. Technical triplicates were used. Cells were left to adhere for about 1 hour at 37°C. Cells were washed with PBS to wash away non-adherent cells, then fixed with 4% PFA for 20minutes. Cells were washed with distilled water then stained with 0.1% crystal violet in 2% ethanol for 60 minutes at room temperature. Cells were washed then incubated with 10% acetic acid on a shaker for 5 minutes. Absorbance was measured at 570nm.

Urine

Albumin was measured using a mouse albumin ELISA kit (Bethyl Laboratories Inc) and creatinine was measured on the Konelab Prime 60i Analyzer.

Blood tests

Mouse plasma was processed either using the Konelab Prime 60i analyzer or the Roche Cobas system with reagents and protocols supplied by the manufacturer.

Histology

3μm paraffin sections stained with Hematoxylin & Eosin, Masson's Trichrome and Periodic Acid Schiff Stain were analyzed and scored blindly by a Consultant Histopathologist. The total number of glomeruli was counted, as well as the numbers of globally sclerosed glomeruli, segmentally sclerosed glomeruli, glomeruli with mesangial hypercellularity (glomerulus with at least one mesangial area containing more than three nuclei) and the proportion of interstitium with interstitial fibrosis. Mesangial hypercellularity here was defined as any glomerulus with at least one mesangial area containing more than three nuclei at x10 magnification.

For electron micrographs, Fiji *(65)* was used to quantify the number of foot processes per micron GBM, by overlaying a one micron grid over the images and counting the number of foot processes per micron GBM over the entire image.

Statistical analysis

All data is presented as mean±SEM unless stated otherwise. Each dot represents a biological replicate. Statistical analyses were performed in GraphPad Prism versions 8 and 9 (Graphpad software). Statistical tests used include two-tailed t-test, one-way analysis of variance (ANOVA) with Dunnetts's multiple comparison post hoc analysis, two-way ANOVA with Tukey's multiple comparison post hoc analysis, and Logrank (Mantel-Cox) test for survival analysis.

List of SUPPLEMENTARY MATERIALS

Materials and Methods
Figures S1 to S2
Tables S1 to S3
Data file S1
(66)

REFERENCES

1. A. C. Nathwani, E. G. D. Tuddenham, S. Rangarajan, C. Rosales, J. McIntosh, D. C. Linch, P. Chowdary, A. Riddell, A. J. Pie, C. Harrington, J. O'Beirne, K. Smith, J. Pasi, B. Glader, P. Rustagi, C. Y. C. Ng, M. A. Kay, J. Zhou, Y. Spence, C. L. Morton, J. Allay, J. Coleman, S. Sleep, J. M. Cunningham, D. Srivastava, E. Basner-Tschakarjan, F. Mingozzi, K. A. High, J. T. Gray, U. M. Reiss, A. W. Nienhuis, A. M. Davidoff, Adenovirus-associated virus vector-mediated gene transfer in hemophilia B. *N Engl J Med* **365**, 2357–65 (2011).

2. P. Chowdary, S. Shapiro, M. Makris, G. Evans, S. Boyce, K. Talks, G. Dolan, U. Reiss, M. Phillips, A. Riddell, M. R. Peralta, M. Quaye, D. W. Patch, E. Tuddenham, A. Dane, M. Watissée, A. Long, A. Nathwani, Phase 1–2 Trial of AAVS3 Gene Therapy in Patients with Hemophilia B. *New England Journal of Medicine* **387**, 237–247 (2022).

3. M. C. Ozelo, J. Mahlangu, K. J. Pasi, A. Giermasz, A. D. Leavitt, M. Laffan, E. Symington, D. v. Quon, J.-D. Wang, K. Peerlinck, S. W. Pipe, B. Madan, N. S. Key, G. F. Pierce, B. O'Mahony, R. Kaczmarek, J. Henshaw, A. Lawal, K. Jayaram, M. Huang, X. Yang, W. Y. Wong, B. Kim, Valoctocogene Roxaparvovec Gene Therapy for Hemophilia A. *New England Journal of Medicine* **386**, 1013–1025 (2022).

4. J. W. B. Bainbridge, M. S. Mehat, V. Sundaram, S. J. Robbie, S. E. Barker, C. Ripamonti, A. Georgiadis, F. M. Mowat, S. G. Beattie, P. J. Gardner, K. L. Feathers, V. A. Luong, S. Yzer, K. Balaggan, A. Viswanathan, T. J. L. de Ravel, I. Casteels, G. E. Holder, N. Tyler, F. W. Fitzke, R. G. Weleber, M. Nardini, A. T. Moore, D. A. Thompson, S. M. Petersen-Jones, M. Michaelides, L. I. van den Born, A. Stockman, A. J. Smith, G. Rubin, R. R. Ali, Long-term effect of gene therapy on Leber's congenital amaurosis. *N Engl J Med* **372**, 1887–97 (2015).

5. J. R. Mendell, S. Al-Zaidy, R. Shell, W. D. Arnold, L. R. Rodino-Klapac, T. W. Prior, L. Lowes, L. Alfano, K. Berry, K. Church, J. T. Kissel, S. Nagendran, J. L'Italien, D. M. Sproule, C. Wells, J. A. Cardenas, M. D. Heitzer, A. Kaspar, S. Corcoran, L. Braun, S. Likhite, C. Miranda, K. Meyer, K. D. Foust, A. H. M. Burghes, B. K. Kaspar, Single-Dose Gene-Replacement Therapy for Spinal Muscular Atrophy. *New England Journal of Medicine* **377**, 1713–1722 (2017).

6. A. C. Nathwani, U. M. Reiss, E. G. D. Tuddenham, C. Rosales, P. Chowdary, J. Mcintosh, M. Della Peruta, E. Lheriteau, N. Patel, D. Raj, A. Riddell, J. Pie, S. Rangarajan, D. Bevan, M. Recht, Y.-M. Shen, K. G. Halka, E. Basner-Tschakarjan, F. Mingozzi, K. A. High, J. Allay, M. A. Kay, C. Y. C. Ng, J. Zhou, M. Cancio, C. L. Morton, J. T. Gray, D. Srivastava, A. W. Nienhuis, A. M. Davidoff, Long-Term Safety and Efficacy of Factor IX Gene Therapy in Hemophilia B. *N Engl J Med* **21371**, 1994–2004 (2014).

7. C. Zincarelli, S. Soltys, G. Rengo, J. E. Rabinowitz, Analysis of AAV serotypes 1-9 mediated gene expression and tropism in mice after systemic injection. *Mol Ther* **16**, 1073–80 (2008).

8. J. S. Sénac, R. J. Chandler, J. R. Sysol, L. Li, C. P. Venditti, Gene therapy in a murine model of methylmalonic acidemia using rAAV9-mediated gene delivery. *Gene Ther* **19**, 385–91 (2012).

9. C. J. Rocca, S. N. Ur, F. Harrison, S. Cherqui, rAAV9 combined with renal vein injection is optimal for kidney-targeted gene delivery: conclusion of a comparative study. *Gene Ther* **21**, 618–28 (2014).

10. J. L. Picconi, M. a Muff-Luett, D. Wu, E. Bunchman, F. Schaefer, P. D. Brophy, Kidney-specific expression of GFP by in-utero delivery of pseudotyped adeno-associated virus 9. *Mol Ther Methods Clin Dev* **1**, 14014 (2014).

11. S. Chen, A. Agarwal, O. Y. Glushakova, M. S. Jorgensen, S. K. Salgar, A. Poirier, T. R. Flotte, B. P. Croker, K. M. Madsen, M. A. Atkinson, W. W. Hauswirth, K. I. Berns, C. C. Tisher, Gene delivery in renal tubular epithelial cells using recombinant adeno-associated viral vectors. *J Am Soc Nephrol* **14**, 947–58 (2003).

12. S. Schievenbusch, I. Strack, M. Scheffler, R. Nischt, O. Coutelle, M. Hösel, M. Hallek, J. W. U. Fries, H.-P. Dienes, M. Odenthal, H. Büning, Combined paracrine and endocrine AAV9 mediated expression of hepatocyte growth factor for the treatment of renal fibrosis. *Mol Ther* **18**, 1302–9 (2010).

13. X. Luo, G. Hall, S. Li, A. Bird, P. J. Lavin, M. P. Winn, A. R. Kemper, T. T. Brown, D. D. Koeberl, Hepatorenal correction in murine glycogen storage disease type I with a double-stranded adeno-associated virus vector. *Mol Ther* **19**, 1961–70 (2011).

14. J. Zhao, Y. Yue, A. Patel, L. Wasala, J. F. Karp, K. Zhang, D. Duan, Y. Lai, High-Resolution Histological Landscape of AAV DNA Distribution in Cellular Compartments and Tissues following Local and Systemic Injection. *Mol Ther Methods Clin Dev* **18**, 856–868 (2020).

15. J. F. Lang, S. A. Toulmin, K. L. Brida, L. C. Eisenlohr, B. L. Davidson, Standard screening methods underreport AAV-mediated transduction and gene editing. *Nat Commun* **10**, 1–10 (2019).

16. Y. Ikeda, Z. Sun, X. Ru, L. H. Vandenberghe, B. D. Humphreys, Efficient Gene Transfer to Kidney Mesenchymal Cells Using a Synthetic Adeno-Associated Viral Vector. *J Am Soc Nephrol* **29**, 2287–2297 (2018).

17. W. Y. Ding, M. A. Saleem, Current concepts of the podocyte in nephrotic syndrome. *Kidney Res Clin Pract* (2012).

18. A. Bierzynska, H. J. McCarthy, K. Soderquest, E. S. Sen, E. Colby, W. Y. Ding, M. M. Nabhan, L. Kerecuk, S. Hegde, D. Hughes, S. Marks, S. Feather, C. Jones, N. J. A. Webb, M. Ognjanovic, M. Christian, R. D. Gilbert, M. D. Sinha, G. M. Lord, M. Simpson, A. B. Koziell, G. I. Welsh, M. A. Saleem, Genomic and clinical profiling of a national nephrotic syndrome cohort advocates a precision medicine approach to disease management. *Kidney Int* **91**, 937–947 (2017).

19. C. E. Sadowski, S. Lovric, S. Ashraf, W. L. Pabst, H. Y. Gee, S. Kohl, S. Engelmann, V. Vega-Warner, H. Fang, J. Halbritter, M. J. Somers, W. Tan, S. Shril, I. Fessi, R. P. Lifton, D. Bockenhauer, S. El-Desoky, J. A. Kari, M. Zenker, M. J. Kemper, D. Mueller, H. M. Fathy, N. A. Soliman, F. Hildebrandt, F. Hildebrandt, A Single-Gene Cause in 29.5% of Cases of Steroid-Resistant Nephrotic Syndrome. *Journal of the American Society of Nephrology* **26**, 1279–1289 (2015).

20. A. Trautmann, M. Bodria, F. Ozaltin, A. Gheisari, A. Melk, M. Azocar, A. Anarat, S. Caliskan, F. Emma, J. Gellermann, J. Oh, E. Baskin, J. Ksiazek, G. Remuzzi, O. Erdogan, S. Akman, J. Dusek, T. Davitaia, O. Özkaya, F. Papachristou, A. Firszt-Adamczyk, T. Urasinski, S. Testa, R. T. Krmar, L. Hyla-Klekot, A. Pasini, Z. B. Özcakar, P. Sallay, N. Cakar, M. Galanti, J. Terzic, B. Aoun, A. C. Afonso, H. Szymanik-Grzelak, B. S. Lipska, S. Schnaidt, F. Schaefer, Spectrum of steroid-resistant and congenital nephrotic syndrome in children: The podoNet registry cohort. *Clinical Journal of the American Society of Nephrology* **10**, 592–600 (2015).

21. K. Bouchireb, O. Boyer, O. Gribouval, F. Nevo, E. Huynh-Cong, V. Morinière, R. Campait, E. Ars, D. Brackman, J. Dantal, P. Eckart, M. Gigante, B. S. Lipska, A. Liutkus, A. Megarbane, N. Mohsin, F. Ozaltin, M. A. Saleem, F. Schaefer, K. Soulami, R. Torra, N. Garcelon, G. Mollet, K. Dahan, C. Antignac, NPHS2 mutations in steroid-resistant nephrotic syndrome: A mutation update and the associated phenotypic spectrum. *Hum Mutat* **35**, 178–186 (2014).

22. M. C. Starr, I. J. Chang, L. S. Finn, A. Sun, A. A. Larson, J. Goebel, C. Hanevold, J. Thies, J. L. K. Van Hove, S. R. Hingorani, C. Lam, COQ2 nephropathy: a treatable cause of nephrotic syndrome in children. *Pediatr Nephrol* **33**, 1257–1261 (2018).

23. S. F. Heeringa, G. Chernin, M. Chaki, W. Zhou, A. J. Sloan, Z. Ji, L. X. Xie, L. Salviati, T. W. Hurd, V. Vega-Warner, P. D. Killen, Y. Raphael, S. Ashraf, B. Ovunc, D. S. Schoeb, H. M. McLaughlin, R. Airik, C. N. Vlangos, R. Gbadegesin, B. Hinkes, P. Saisawat, E. Trevisson, M. Doimo,

A. Casarin, V. Pertegato, G. Giorgi, H. Prokisch, A. Rötig, G. Nürnberg, C. Becker, S. Wang, F. Ozaltin, R. Topaloglu, A. Bakkaloglu, S. A. Bakkaloglu, D. Müller, A. Beissert, S. Mir, A. Berdeli, S. Varpizen, M. Zenker, V. Matejas, C. Santos-Ocaña, P. Navas, T. Kusakabe, A. Kispert, S. Akman, N. A. Soliman, S. Krick, P. Mundel, J. Reiser, P. Nürnberg, C. F. Clarke, R. C. Wiggins, C. Faul, F. Hildebrandt, COQ6 mutations in human patients produce nephrotic syndrome with sensorineural deafness. *J Clin Invest* **121**, 2013–24 (2011).

24. G. Montini, C. Malaventura, L. Salviati, Early Coenzyme Q10 Supplementation in Primary Coenzyme Q10 Deficiency. *New England Journal of Medicine* **358**, 2849–2850 (2008).

25. N. Boute, O. Gribouval, S. Roselli, F. Benessy, H. Lee, A. Fuchshuber, K. Dahan, M. C. Gubler, P. Niaudet, C. Antignac, NPHS2, encoding the glomerular protein podocin, is mutated in autosomal recessive steroid-resistant nephrotic syndrome. *Nat Genet* **24**, 349–54 (2000).

26. K. Schwarz, M. Simons, J. Reiser, M. A. Saleem, C. Faul, W. Kriz, A. S. Shaw, L. B. Holzman, P. Mundel, Podocin , a raft-associated component of the glomerular slit diaphragm , interacts with CD2AP and nephrin. *J Clin Invest* **108**, 1583–1587 (2001).

27. T. B. Huber, B. Schermer, T. Benzing, Podocin organizes ion channel-lipid supercomplexes: implications for mechanosensation at the slit diaphragm. *Nephron Exp Nephrol* **106**, e27-31 (2007).

28. S. Roselli, I. Moutkine, O. Gribouval, A. Benmerah, C. Antignac, Plasma Membrane Targeting of Podocin Through the Classical Exocytic Pathway: Effect of NPHS2 Mutations. *Traffic* **5**, 37–44 (2004).

29. G. Mollet, J. Ratelade, O. Boyer, A. O. Muda, L. Morisset, T. A. Lavin, D. Kitzis, M. J. Dallman, L. Bugeon, N. Hubner, M.-C. Gubler, C. Antignac, E. L. Esquivel, Podocin inactivation in mature kidneys causes focal segmental glomerulosclerosis and nephrotic syndrome. *J Am Soc Nephrol* **20**, 2181–9 (2009).

30. M. Tabatabaeifar, T. Wlodkowski, I. Simic, H. Denc, G. Mollet, S. Weber, J. J. Moyers, B. Brühl, M. J. Randles, R. Lennon, C. Antignac, F. Schaefer, An inducible mouse model of podocin-mutation-related nephrotic syndrome. *PLoS One* **12**, 1–21 (2017).

31. M. a Wong, S. Cui, S. E. Quaggin, Identification and characterization of a glomerular-specific promoter from the human nephrin gene. *Am J Physiol Renal Physiol* **279**, F1027-32 (2000).

32. M. I. Patrício, A. R. Barnard, H. O. Orlans, M. E. McClements, R. E. MacLaren, Inclusion of the Woodchuck Hepatitis Virus Posttranscriptional Regulatory Element Enhances AAV2-Driven Transduction of Mouse and Human Retina. *Mol Ther Nucleic Acids* **6**, 198–208 (2017).

33. R. Klein, B. Ruttkowski, E. Knapp, B. Salmons, W. H. Günzburg, C. Hohenadl, WPRE-mediated enhancement of gene expression is promoter and cell line specific. *Gene* **372**, 153–161 (2006).

34. A. Schambach, J. Bohne, C. Baum, F. G. Hermann, L. Egerer, D. von Laer, T. Giroglou, Woodchuck hepatitis virus post-transcriptional regulatory element deleted from X protein and promoter sequences enhances retroviral vector titer and expression. *Gene Ther* **13**, 641–5 (2006).

35. R. E. MacLaren, M. Groppe, A. R. Barnard, C. L. Cottriall, T. Tolmachova, L. Seymour, K. R. Clark, M. J. During, F. P. M. Cremers, G. C. M. Black, A. J. Lotery, S. M. Downes, A. R. Webster, M. C. Seabra, Retinal gene therapy in patients with choroideremia: initial findings from a phase 1/2 clinical trial. *Lancet* **383**, 1129–37 (2014).

36. J. J. Harris, H. J. McCarthy, L. Ni, M. Wherlock, H. Kang, J. F. Wetzels, G. I. Welsh, M. a Saleem, Active proteases in nephrotic plasma lead to a podocin-dependent phosphorylation of VASP in podocytes via protease activated receptor-1. *J Pathol* **229**, 660–71 (2013).

37. A. Philippe, S. Weber, E. L. Esquivel, C. Houbron, G. Hamard, J. Ratelade, W. Kriz, F. Schaefer, M.-C. Gubler, C. Antignac, A missense mutation in podocin leads to early and severe renal disease in mice. *Kidney Int* **73**, 1038–1047 (2008).

38. L. Lisowski, A. P. Dane, K. Chu, Y. Zhang, S. C. Cunningham, E. M. Wilson, S. Nygaard, M. Grompe, I. E. Alexander, M. a Kay, Selection and evaluation of clinically relevant AAV variants in a xenograft liver model. *Nature* (2013), doi:10.1038/nature12875.

39. E. A. Rutledge, C. L. Halbert, D. W. Russell, *Infectious Clones and Vectors Derived from Adeno-Associated Virus (AAV) Serotypes Other Than AAV Type 2* (1998; https://journals.asm.org/journal/jvi).

40. C. Ling, Y. Lu, J. K. Kalsi, G. R. Jayandharan, B. Li, W. Ma, B. Cheng, S. W. Y. Gee, K. E. McGoogan, L. Govindasamy, L. Zhong, M. Agbandje-Mckenna, A. Srivastava, Human hepatocyte growth factor receptor is a cellular coreceptor for adeno-associated virus serotype 3. *Hum Gene Ther* **21**, 1741–1747 (2010).

41. C. Dai, M. A. Saleem, L. B. Holzman, P. Mathieson, Y. Liu, Hepatocyte growth factor signaling ameliorates podocyte injury and proteinuria. *Kidney Int* **77**, 962–973 (2010).

42. C. Schell, T. B. Huber, The Evolving Complexity of the Podocyte Cytoskeleton. *J Am Soc Nephrol* **28**, 3166–3174 (2017).

43. S. Ashraf, H. Kudo, J. Rao, A. Kikuchi, E. Widmeier, J. A. Lawson, W. Tan, T. Hermle, J. K. Warejko, S. Shril, M. Airik, T. Jobst-Schwan, S. Lovric, D. A. Braun, H. Y. Gee, D. Schapiro, A. J. Majmundar, C. E. Sadowski, W. L. Pabst, A. Daga, A. T. van der Ven, J. M. Schmidt, B. C. Low, A.

B. Gupta, B. K. Tripathi, J. Wong, K. Campbell, K. Metcalfe, D. Schanze, T. Niihori, H. Kaito, K. Nozu, H. Tsukaguchi, R. Tanaka, K. Hamahira, Y. Kobayashi, T. Takizawa, R. Funayama, K. Nakayama, Y. Aoki, N. Kumagai, K. Iijima, H. Fehrenbach, J. A. Kari, S. El Desoky, S. Jalalah, R. Bogdanovic, N. Stajić, H. Zappel, A. Rakhmetova, S.-R. Wassmer, T. Jungraithmayr, J. Strehlau, A. S. Kumar, A. Bagga, N. A. Soliman, S. M. Mane, L. Kaufman, D. R. Lowy, M. A. Jairajpuri, R. P. Lifton, Y. Pei, M. Zenker, S. Kure, F. Hildebrandt, Mutations in six nephrosis genes delineate a pathogenic pathway amenable to treatment. *Nat Commun* **9**, 1960 (2018).

44. L. K. Farmer, R. Rollason, D. J. Whitcomb, L. Ni, A. Goodliff, A. C. Lay, L. Birnbaumer, K. J. Heesom, S. Z. Xu, M. A. Saleem, G. I. Welsh, TRPC6 Binds to and activates calpain, independent of its channel activity, and regulates podocyte cytoskeleton, cell adhesion, and motility. *Journal of the American Society of Nephrology* **30**, 1910–1924 (2019).

45. B. L. Wharram, M. Goyal, J. E. Wiggins, S. K. Sanden, S. Hussain, W. E. Filipiak, T. L. Saunders, R. C. Dysko, K. Kohno, L. B. Holzman, R. C. Wiggins, Podocyte depletion causes glomerulosclerosis: Diphtheria toxin-induced podocyte depletion in rats expressing human diphtheria toxin receptor transgene. *Journal of the American Society of Nephrology* **16**, 2941–2952 (2005).

46. D. P. Perocheau, S. C. Cunningham, J. Lee, J. Antinao Diaz, S. N. Waddington, K. Gilmour, S. Eaglestone, L. Lisowski, A. J. Thrasher, I. E. Alexander, P. Gissen, J. Baruteau, Age-Related Seroprevalence of Antibodies Against AAV-LK03 in a UK Population Cohort. *Hum Gene Ther* **30**, 79–87 (2019).

47. C. Hopkins, J. Li, F. Rae, M. Little, Stem cell options for kidney disease. *J Pathol* **217**, 265–281 (2009).

48. E. Ronconi, C. Sagrinati, M. L. Angelotti, E. Lazzeri, B. Mazzinghi, L. Ballerini, E. Parente, F. Becherucci, M. Gacci, M. Carini, E. Maggi, M. Serio, G. B. Vannelli, L. Lasagni, S. Romagnani, P. Romagnani, Regeneration of glomerular podocytes by human renal progenitors. *J Am Soc Nephrol* **20**, 322–32 (2009).

49. D. Appel, D. B. Kershaw, B. Smeets, G. Yuan, A. Fuss, B. Frye, M. Elger, W. Kriz, J. Floege, M. J. Moeller, Recruitment of podocytes from glomerular parietal epithelial cells. *J Am Soc Nephrol* **20**, 333–43 (2009).

50. J. B. Kopp, G. W. Nelson, K. Sampath, R. C. Johnson, G. Genovese, P. An, D. Friedman, W. Briggs, R. Dart, S. Korbet, M. H. Mokrzycki, P. L. Kimmel, S. Limou, T. S. Ahuja, J. S. Berns, J. Fryc, E. E. Simon, M. C. Smith, H. Trachtman, D. M. Michel, J. R. Schelling, D. Vlahov, M. Pollak, C. A. Winkler, APOL1 genetic variants in focal segmental glomerulosclerosis and HIV-associated nephropathy. *J Am Soc Nephrol* **22**, 2129–37 (2011).

51. S. C. Satchell, F. Braet, Glomerular endothelial cell fenestrations: an integral component of the glomerular filtration barrier. *Am J Physiol Renal Physiol* **296**, F947-56 (2009).

52. A. C. Nathwani, C. Rosales, J. McIntosh, G. Rastegarlari, D. Nathwani, D. Raj, S. Nawathe, S. N. Waddington, R. Bronson, S. Jackson, R. E. Donahue, K. A. High, F. Mingozzi, C. Y. C. Ng, J. Zhou, Y. Spence, M. B. McCarville, M. Valentine, J. Allay, J. Coleman, S. Sleep, J. T. Gray, A. W. Nienhuis, A. M. Davidoff, Long-term safety and efficacy following systemic administration of a self-complementary AAV vector encoding human FIX pseudotyped with serotype 5 and 8 capsid proteins. *Molecular Therapy* **19**, 876–885 (2011).

53. R. Ferla, M. Alliegro, J. B. Marteau, M. Dell'Anno, E. Nusco, S. Pouillot, S. Galimberti, M. G. Valsecchi, V. Zuliani, A. Auricchio, Non-clinical Safety and Efficacy of an AAV2/8 Vector Administered Intravenously for Treatment of Mucopolysaccharidosis Type VI. *Mol Ther Methods Clin Dev* **6**, 143–158 (2017).

54. C. N. Mattar, A. M. S. S. Wong, K. Hoefer, M. E. Alonso-Ferrero, S. M. K. K. Buckley, S. J. Howe, J. D. Cooper, S. N. Waddington, J. K. Y. Y. Chan, A. A. Rahim, Systemic gene delivery following intravenous administration of AAV9 to fetal and neonatal mice and late-gestation nonhuman primates. *FASEB Journal* **29**, 3876–3888 (2015).

55. V. Eremina, M. A. Wong, S. Cui, L. Schwartz, S. E. Quaggin, Evaluation of a New Tool for Exploring Podocyte Biology: Mouse Nphs1 5' Flanking Region Drives LacZ Expression in Podocytes. *Journal of the American Society of Nephrology* **11**, 2306–2314 (2002).

56. D. R. Deyle, D. W. Russell, Adeno-associated virus vector integration. *Curr Opin Mol Ther* **11**, 442–447 (2009).

57. F. Mingozzi, K. A. High, Overcoming the Host Immune Response to Adeno-Associated Virus Gene Delivery Vectors: The Race Between Clearance, Tolerance, Neutralization, and Escape. *Annu Rev Virol* **4**, 511–534 (2017).

58. S. Zolotukhin, B. Byrne, E. Mason, I. Zolotukhin, M. Potter, K. Chesnut, C. Summerford, R. Samulski, N. Muzyczka, Recombinant adeno-associated virus purification using novel methods improves infectious titer and yield. *Gene Ther* **6**, 973–985 (1999).

59. J. Juhila, R. Roozendaal, M. Lassila, S. J. Verbeek, H. Holthofer, Podocyte cell-specific expression of doxycycline inducible Cre recombinase in mice. *J Am Soc Nephrol* **17**, 648–54 (2006).

60. M. A. Saleem, M. J. O'Hare, J. Reiser, R. J. Coward, C. D. Inward, T. Farren, C. Y. Xing, L. Ni, P. W. Mathieson, P. Mundel, A conditionally immortalized human podocyte cell line demonstrating nephrin and podocin expression. *J Am Soc Nephrol* **13**, 630–8 (2002).

61. L. NI, M. SALEEM, P. W. MATHIESON, Podocyte culture: Tricks of the trade. *Nephrology* **17**, 525–531 (2012).

62. J. A. Hurcombe, P. Hartley, A. C. Lay, L. Ni, J. J. Bedford, J. P. Leader, S. Singh, A. Murphy, C. L. Scudamore, E. Marquez, A. F. Barrington, V. Pinto, M. Marchetti, L. F. Wong, J. Uney, M. A. Saleem, P. W. Mathieson, S. Patel, R. J. Walker, J. R. Woodgett, S. E. Quaggin, G. I. Welsh, R. J. M. Coward, Podocyte GSK3 is an evolutionarily conserved critical regulator of kidney function. *Nature Communications 2019 10:1* **10**, 1–17 (2019).

63. S. C. C. Satchell, C. H. H. Tasman, A. Singh, L. Ni, J. Geelen, C. J. J. von Ruhland, M. J. J. O'Hare, M. A. A. Saleem, L. P. P. van den Heuvel, P. W. W. Mathieson, Conditionally immortalized human glomerular endothelial cells expressing fenestrations in response to VEGF. *Kidney Int* **69**, 1633–40 (2006).

64. M. J. Wilmer, M. A. Saleem, R. Masereeuw, L. Ni, T. J. Van Der Velden, F. G. Russel, P. W. Mathieson, L. A. Monnens, L. P. Van Den Heuvel, E. N. Levtchenko, Novel conditionally immortalized human proximal tubule cell line expressing functional influx and efflux transporters. *Cell Tissue Res* **339**, 449 (2010).

65. J. Schindelin, I. Arganda-Carreras, E. Frise, V. Kaynig, M. Longair, T. Pietzsch, S. Preibisch, C. Rueden, S. Saalfeld, B. Schmid, J.-Y. Tinevez, D. J. White, V. Hartenstein, K. Eliceiri, P. Tomancak, A. Cardona, Fiji: an open-source platform for biological-image analysis. *Nat Methods* **9**, 676–682 (2012).

66. D. G. Gibson, L. Young, R.-Y. Chuang, J. C. Venter, C. A. Hutchison, H. O. Smith, Enzymatic assembly of DNA molecules up to several hundred kilobases. *Nat Methods* **6**, 343–345 (2009).

Acknowledgments: Many thanks to K. Stevenson and K. Burt who kindly processed the plasma and urine samples. Flow cytometry was run with the help of L. Suiero Ballesteros and A. Herman. The authors gratefully acknowledge the Wolfson Bioimaging Facility, in particular A. Leard and K. Jepson, for their support and assistance in this work.

Funding: WYD was funded by the Wellcome Trust/ Elizabeth Blackwell Institute Clinical Primer Scheme, Kidney Research UK Clinical Research Training Fellowship (TF7/2015 to WYD) and the NIHR as an Academic Clinical Lecturer. This work was also funded by the Nephrotic Syndrome Trust; grant awards SGL024\1045 from Academy of Medical Sciences to WYD; grant awards ST_004_20151126 and KKR/Paed 2016/01 from Kidney Research UK to GIW; MR/R003017/1 from the Medical Research Council to MAS. RJC was supported with an MRC Senior Research Fellowship (MR/K010492/1).

Author contributions: MAS conceived the idea. WYD, GIW, AN and MAS developed the idea. WYD designed, carried out experiments and analyzed the data. GM, JH, CC, JM, RJC and CA provided critical feedback on experimental design. VK, SH, AL, BH, RR, JH, FB, WC, CM, CJM, JT and TR carried out experiments. MB analysed histological data. WYD wrote the manuscript in consultation with MAS and GIW, with final input from all authors.

Competing interests: MAS and GIW are inventors on a patent family derived from UK Patent Application Number GB1900702.0 and International Patent Application PCT/GB2020/050097, published as WO 2020/148548 (AAV Gene Therapy for Treating Nephrotic Syndrome). VK and JT are employees while GIW and MAS are consultants for Purespring Therapeutics. WYD, GIW and MAS have equity at Purespring Therapeutics.

Data and materials availability: All data associated with this study are in the paper or supplementary materials. Plasmids cloned for this study are available via material transfer agreement (MTA) upon request to Professor Moin Saleem. AAV capsid plasmids (LK03 and 2/9) were obtained via an MTA with the relevant institutions. Mice were obtained via MTAs with the relevant institutions or purchased from Jackson Laboratories.

Figures:

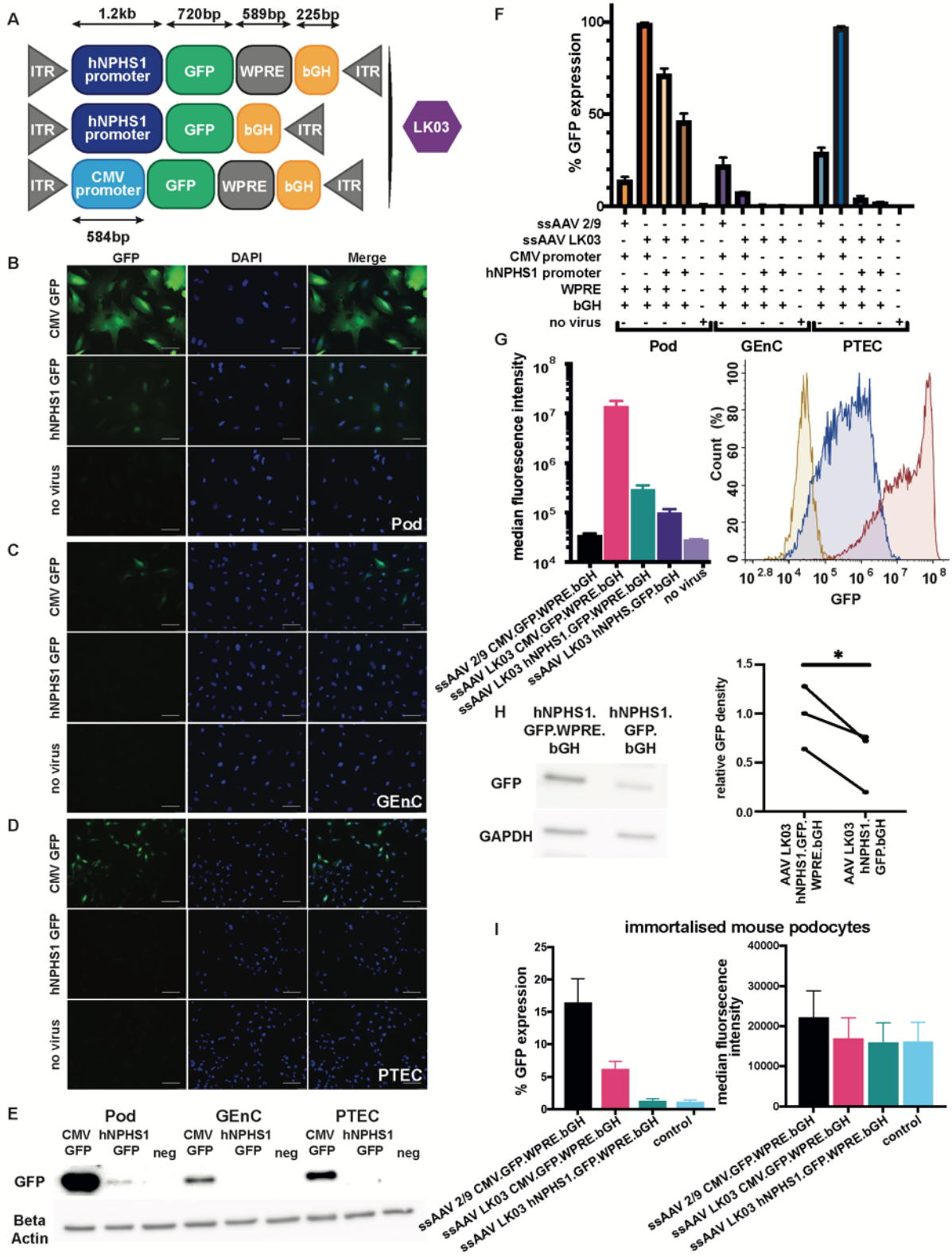

Figure 1. Reciprocal efficacy of AAV-LK03 versus AAV 2/9 on human podocytes versus mouse podocytes in vitro. A) Plasmids pAV.CMV.GFP.WPRE.bGH and pAV.hNPHS1.GFP.WPRE.bGH and pAV.hNPHS1.GFP.bGH were used to produce AAV

LK03 vectors. WPRE=Woodchuck Hepatitis Virus Posttranscriptional Regulatory Element, bGH=bovine growth hormone polyadenylation signal. B to D) Immunofluorescence demonstrating GFP expression of human podocytes (Pod), human glomerular endothelial cells (GEnC) and human proximal tubule epithelial cells (PTEC) transduced by AAV-LK03 CMV GFP and AAV-LK03 hNPHS1 GFP WPRE. Scale bar=100μm. E) Western blot demonstrating GFP expression in human podocytes transduced with AAV-LK03 CMV GFP and AAV-LK03 hNPHS1 GFP WPRE. F) Bar chart of flow cytometry demonstrating GFP expression of Pod, GEnC and PTEC transduced with AAV 2/9 CMV GFP, AAV-LK03 CMV GFP, AAV-LK03 hNPHS1 GFP WPRE and AAV-LK03 hNPHS1 GFP. G) Bar chart (Left) showing median fluorescence intensity in human podocytes transduced with AAV 2/9 CMV GFP, AAV-LK03 CMV GFP, AAV-LK03 hNPHS1 GFP WPRE and AAV-LK03 hNPHS1 GFP (n=3). Histogram (Right) showing the degree of green fluorescence in human podocytes transduced with AAV-LK03 CMV GFP (Red), AAV-LK03 hNPHS1 GFP with WPRE (Blue) and untransduced cells (Yellow). H) Western blot and corresponding densitometry comparing GFP expression of human podocytes transduced with AAV LK03 hNPHS1 GFP with and without WPRE. I) Bar chart of flow cytometry of immortalized mouse podocytes transduced with AAV 2/9 CMV GFP, AAV-LK03 CMV GFP and AAV-LK03 hNPHS1 GFP WPRE. (All flow cytometry experiments minimum n=3)

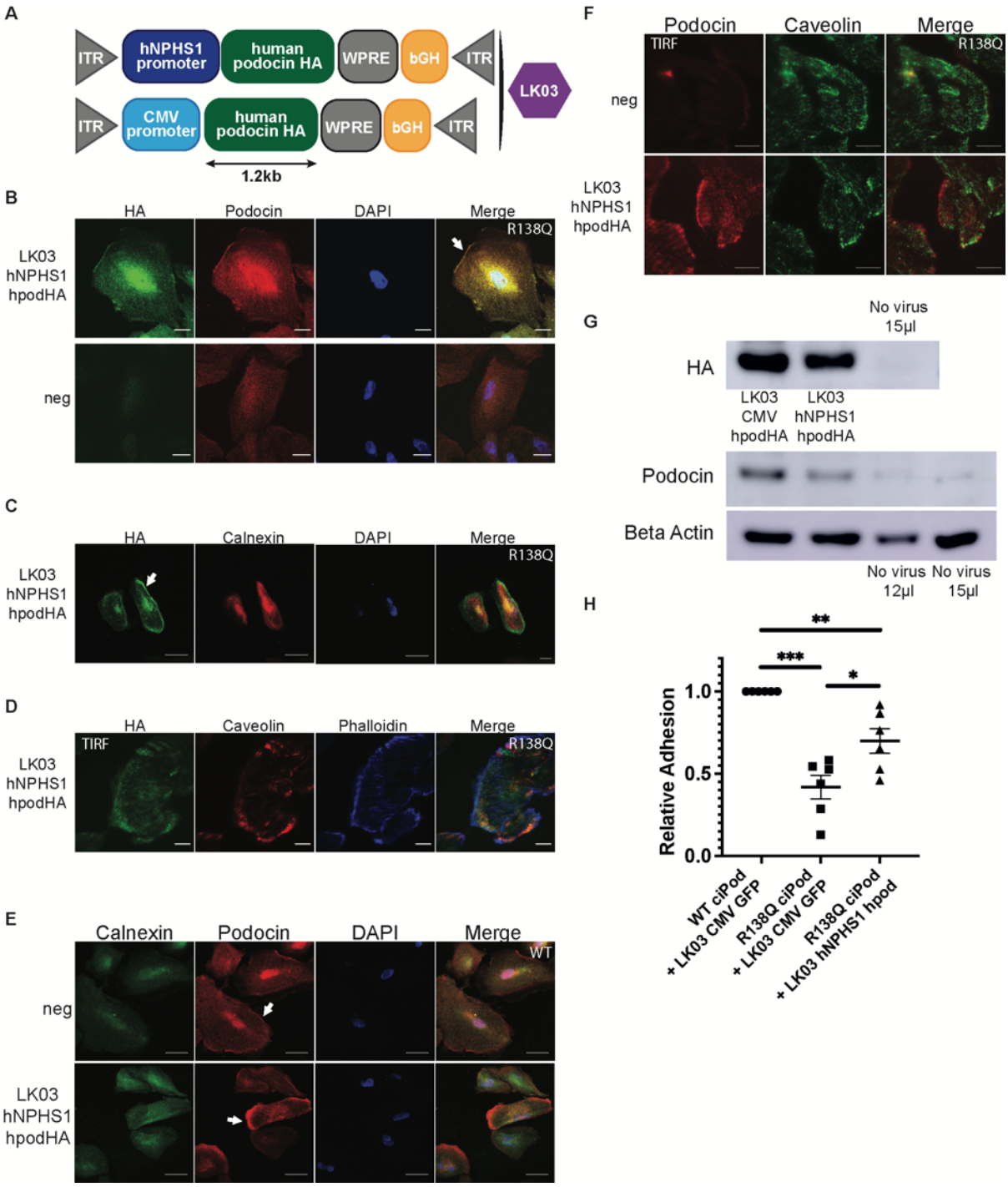

Figure 2. AAV-LK03 expressing wild type human podocin results in functional rescue in vitro the mutant podocin R138Q human podocyte cell line. A) Plasmids pAV.CMV.hpodHA.WPRE.bGH and pAV.hNPHS1.hpodHA.WPRE.bGH were used to produce AAV LK03 vectors. B) Confocal microscopy demonstrating expression of HA-tagged wild type podocin (green) in the mutant podocin R138Q podocytes (White arrow: plasma membrane expression). C) Confocal microscopy showing HA-tagged podocin (white

arrow: plasma membrane expression), and calnexin (red). Nuclei are stained blue. D) TIRF (Total Internal Reflection Fluorescence) microscopy demonstrating expression of HA-tagged podocin (green) and caveolin (red) within 100nm of the plasma membrane. Phalloidin is stained blue. E) Confocal microscopy demonstrating podocin (red)(white arrow: plasma membrane expression) in wild type (WT) podocytes, with or without AAV-LK03.hNPHS1.hpodHA.WPRE.bGH transduction. Calnexin is stained green, nuclei are stained blue. F) TIRF microscopy demonstrating podocin (red) and caveolin (green) in R138Q podocytes, with or without AAV-LK03.hNPHS1.hpodHA.WPRE.bGH transduction. G) Western blot showing HA-tagged podocin in R138Q podocytes, transduced with either AAV-LK03.CMV.hpodHA, AAV-LK03.hNPHS1.hpodHA or no virus. H) Adhesion assay showing adhesion in mutant podocin R138Q podocytes, and wild type human podocytes, transduced with either AAV-LK03.hNPHS1.hpodHA or AAV-LK03 CMV GFP (control virus). (n=6, One-way ANOVA with Tukey's multiple comparisons, *$p<0.05$, **$p<0.01$, ***$p<0.001$) Scale bar=25μm.

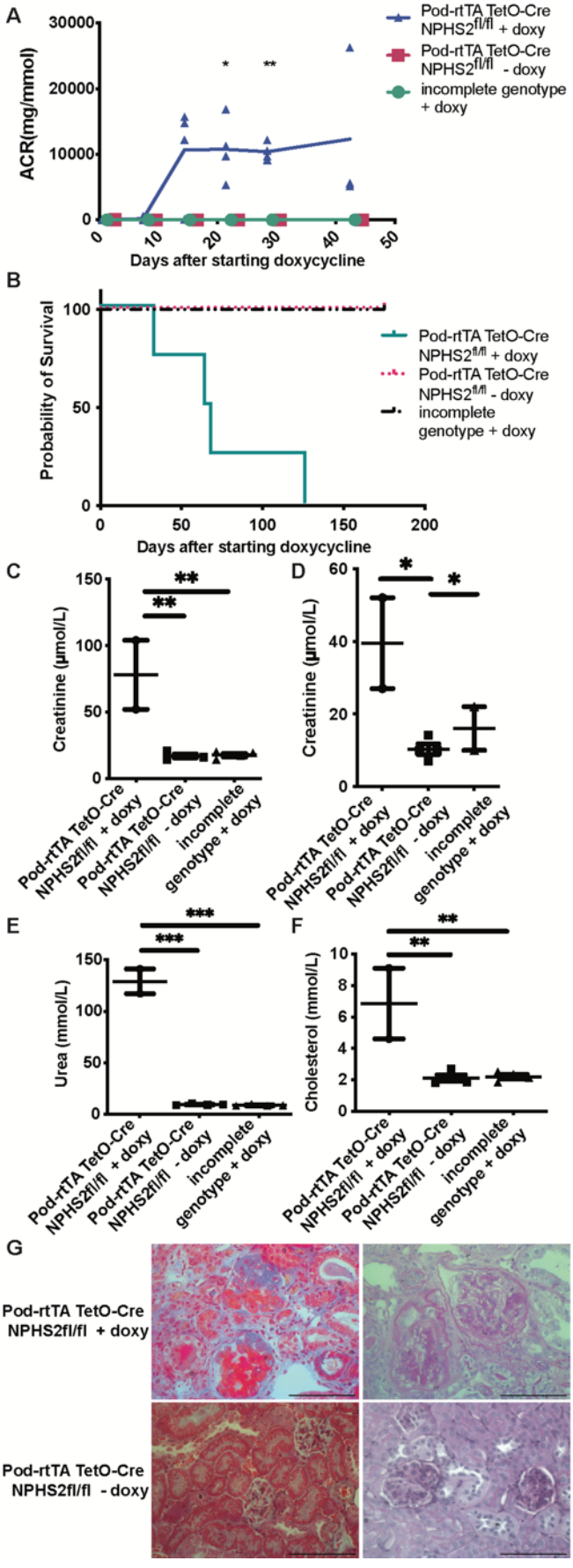

Figure 3. Pod-rtTA TetO-Cre NPHS2$^{fl/fl}$ mice induced with doxycycline develop

nephrotic syndrome. A) Urinary albumin:creatinine ratio (ACR) in Pod-rtTA TetO-Cre NPHS2$^{fl/fl}$ mice, either after doxycycline or without doxycycline administration, and in mice with an incomplete genotype with doxycycline administration (n=4/group). B) Survival curves of Pod-rtTA TetO-Cre NPHS2$^{fl/fl}$ mice, either after doxycycline or without doxycycline administration, and in mice with an incomplete genotype with doxycycline administration. (*n*=2-4/group). Plasma creatinine C) at death and D) at 10 weeks after commencing doxycycline. E) Plasma urea and F) Plasma cholesterol at death. (n=2-4/group) G) Representative images on light microscopy. Masson's Trichrome (collagen stains blue) on left, Periodic Acid Schiff on right (Scale bar=100μm).

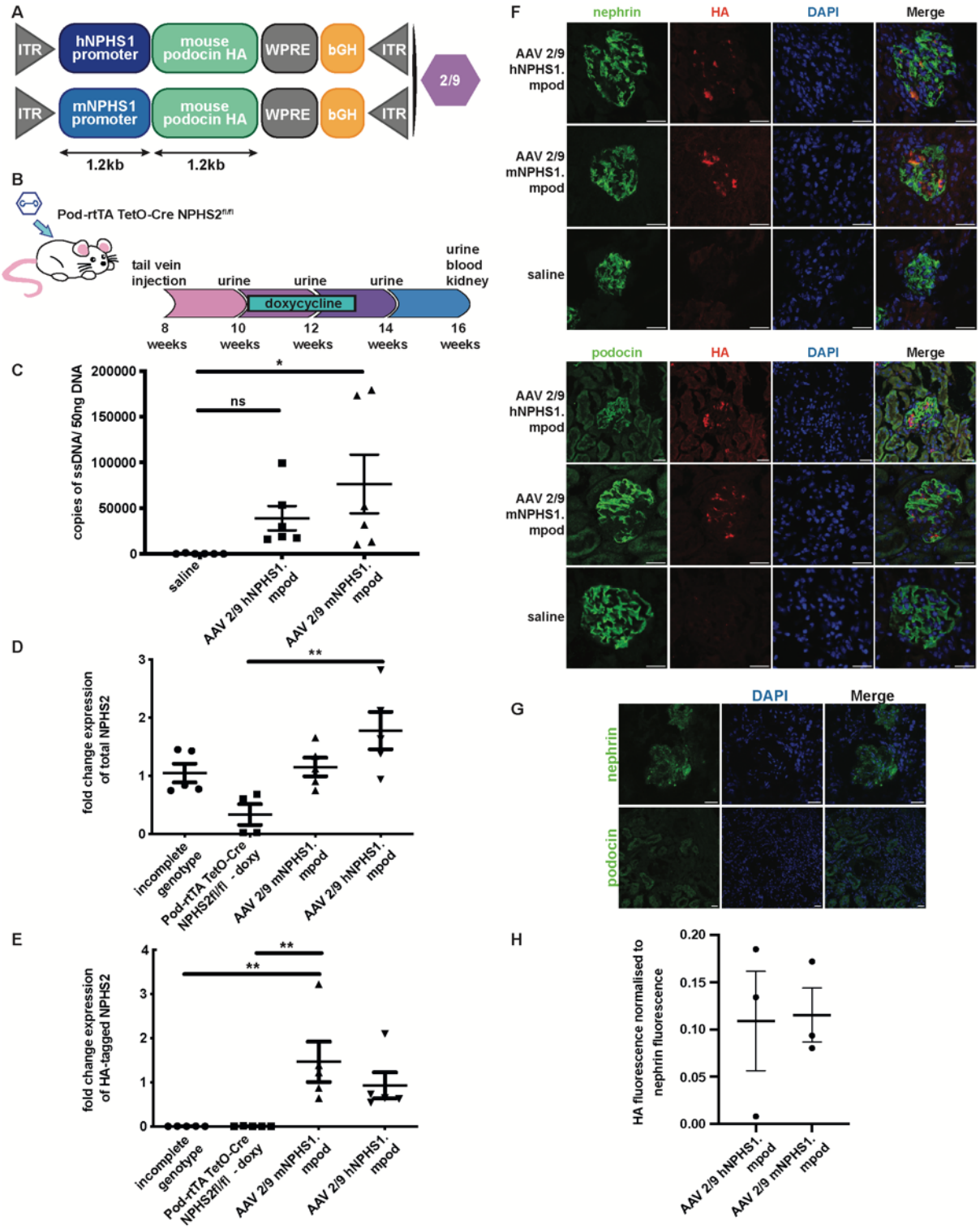

Figure 4. AAV 2/9 administered by tail vein injection transduces the mouse kidney and expresses HA-tagged podocin in the podocyte. A) Plasmids pAV.mNPHS1.mpodHA.WPRE.bGH and pAV.hNPHS1.mpodHA.WPRE.bGH were used to produce AAV 2/9 vectors. B) Vector or saline was injected via tail vein in Pod-rtTA TetO-

Cre NPHS2$^{fl/fl}$ mice at 8 weeks of age, and induction with doxycycline commenced 10 to 14 days later. C) Real-time PCR showing the presence of AAV ITRs in DNA extracted from mouse kidney cortex in mice injected with the viral vector (n = 6 per group, one-way ANOVA with Tukey's multiple comparisons, *P < 0.05). ns, not significant. D) and E) Real-time PCRshowing increased total NPHS2 and HA-tagged podocin mRNA in the mouse kidney tissue of mice injected with the AAV vector (n = 4 to 5 per group, one-way ANOVA with Tukey's multiple comparisons, *P < 0.05, **P < 0.01). ns, not significant. F) Representative immunofluorescence showing expression of HA-tagged podocin with podocyte-specific proteins nephrin and podocin in Pod-rtTA TetO-Cre NPHS2$^{fl/fl}$ mice injected with AAV 2/9. Control (saline) images here are of mice without the full Pod-rtTA TetO-Cre NPHS2$^{fl/fl}$ genotype because mice with diseased glomeruli showed loss or change of podocyte markers. G) Pod-rtTA TetO-Cre NPHS2$^{fl/fl}$ (induced with doxycycline for the full phenotype) mice administered saline demonstrated a change in the pattern of nephrin staining and loss of podocin staining. H) Quantification of HA fluorescence normalized to nephrin fluorescence (n = 3). Scale bar, 25 μm.

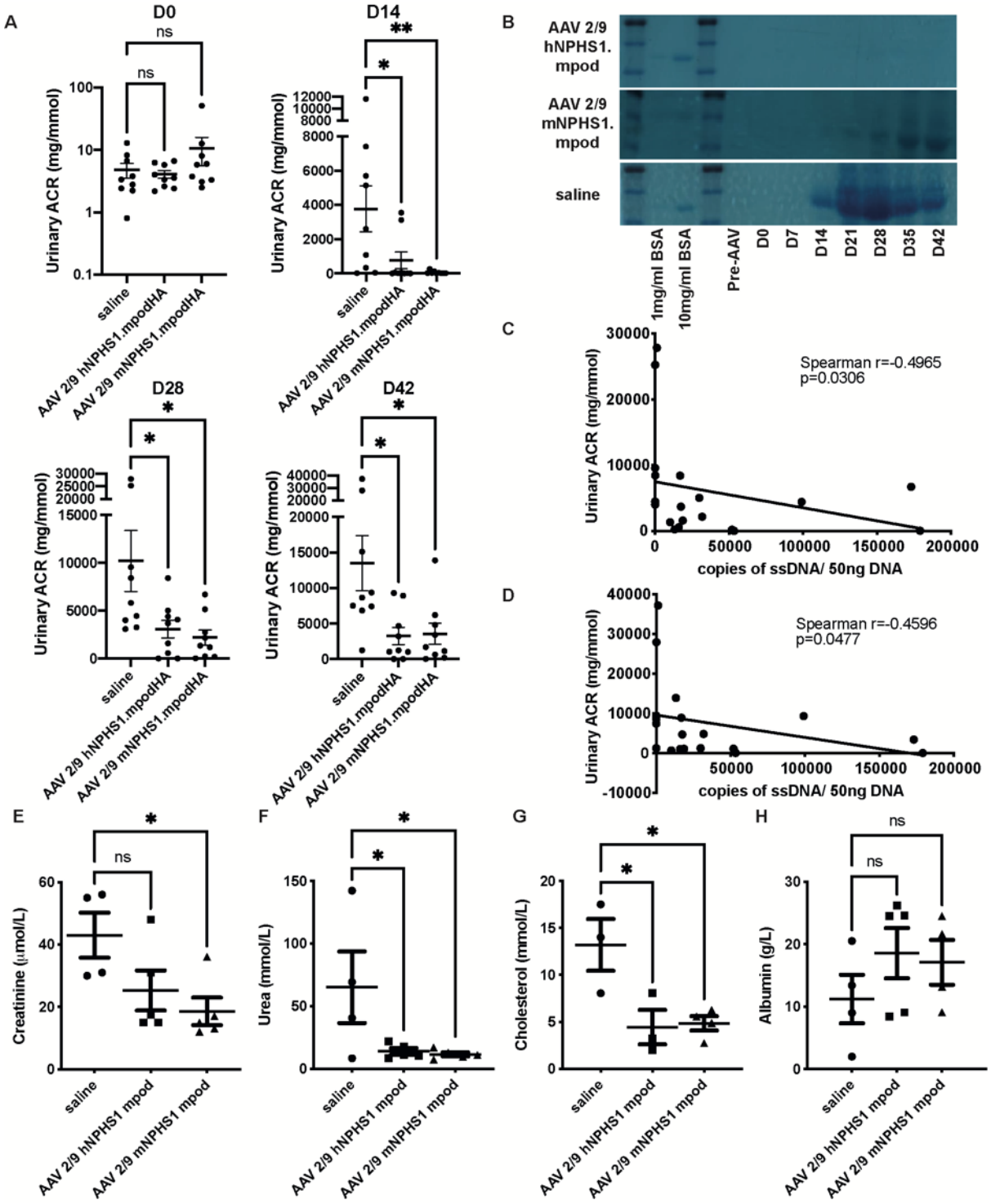

Figure 5. Tail vein injection of AAV 2/9 expressing wild-type podocin under a podocyte-specific promoter before induction of disease reduces proteinuria and improves plasma markers of nephrotic syndrome in the inducible podocin knock-out mouse model (Pod-rtTA TetO-Cre NPHS2$^{fl/fl}$) A) Urinary albumin: creatinine ratio of mice injected with saline versus AAV 2/9 hNPHS1.mpod versus AAV 2/9 mNPHS1.mpod (n=9 in each group, one-

way ANOVA with Dunnett's multiple comparisons, *p<0.05 **p<0.01). B) Coomassie staining showing representative images of degree of albuminuria in a representative mouse from each experimental group. C and D) Correlation of the number of copies of viral DNA per 50ng total DNA with urinary albumin: creatinine ratio at days 28 (C) and 42 (D) (Spearman rank test). Plasma E) creatinine F) urea G) cholesterol and H) albumin from mice at 42 days after start of doxycycline (n=minimum of 3 mice in each group, one-way ANOVA with Dunnett's multiple comparisons, *p<0.05).

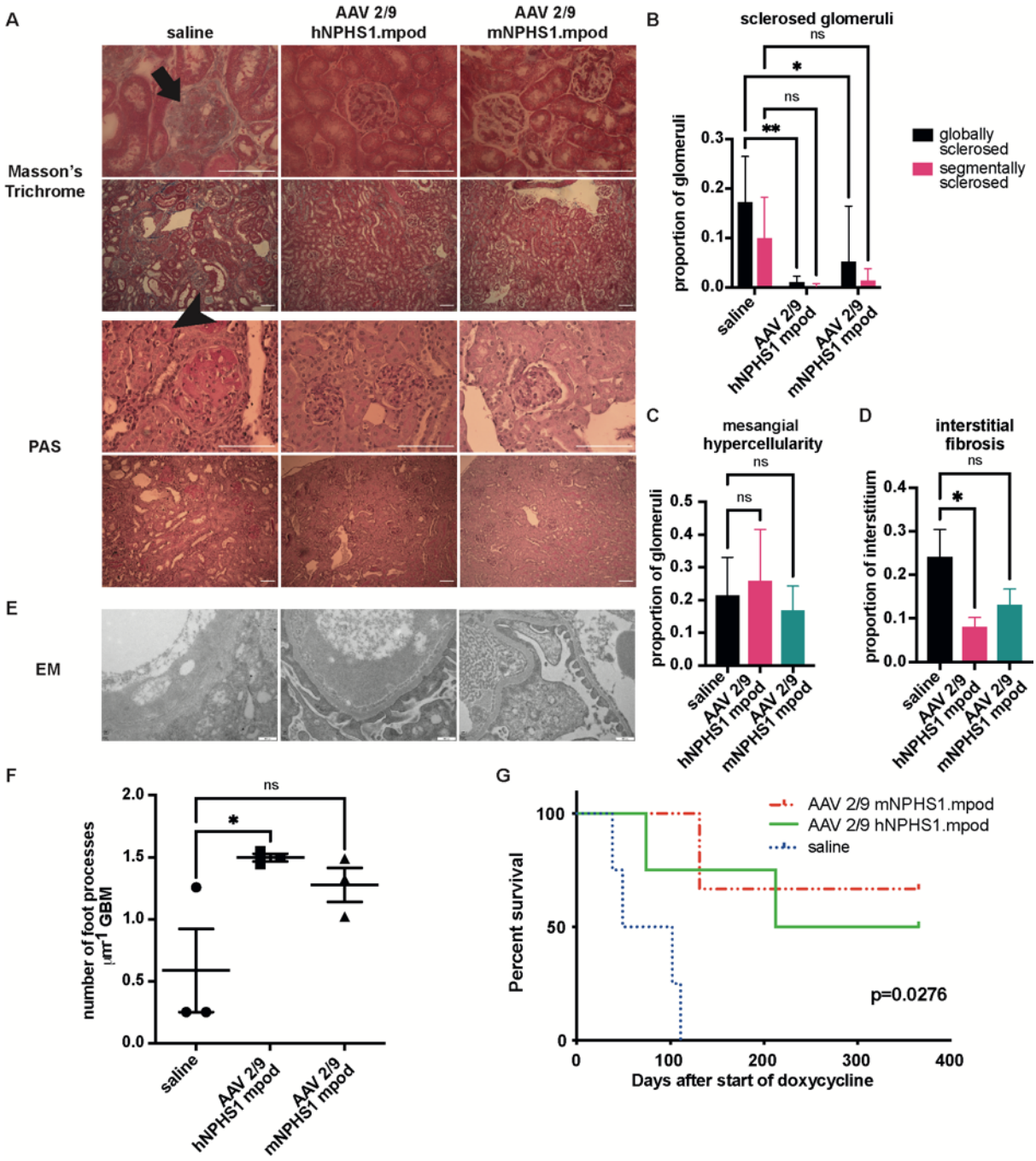

Figure 6. Kidney histology and survival of Pod-rtTA TetO-Cre NPHS2$^{fl/fl}$ mice treated with saline or AAV before induction of disease. A) Representative images on light microscopy. Scale bars=100µm. Black arrow indicates glomerulosclerosis and black arrowhead indicates tubular atrophy. Masson's trichrome shows collagen (blue) while Periodic Acid Schiff (PAS) staining highlights the basement membrane. B) Quantification of the sections in A (n=5-6/group). (Two-way ANOVA with Dunnett's multiple comparisons,

*p<0.05, **p<0.01). Pink=segmentally sclerosed, black=globally sclerosed. C) Quantification of degree of mesangial hypercellularity (One-way ANOVA with Dunnett's multiple comparisons, n=5-6/group). D) Quantification of interstitial fibrosis (One-way ANOVA with Dunnett's multiple comparisons, *p<0.05, n=5-6/group). E) Representative images on electron microscopy. Scale bars=500nm. F) Quantification of number of foot processes per micron glomerular basement membrane on electron micrographs (n=3/group)(One-way ANOVA with Dunnett's multiple comparisons, *p<0.05). G) Survival curves of mice injected with either saline (n=4), AAV 2/9 hNPHS1.mpod (n=4) or AAV 2/9 mNPHS1.mpod (n=3) (Log-rank (Mantel-Cox) test).

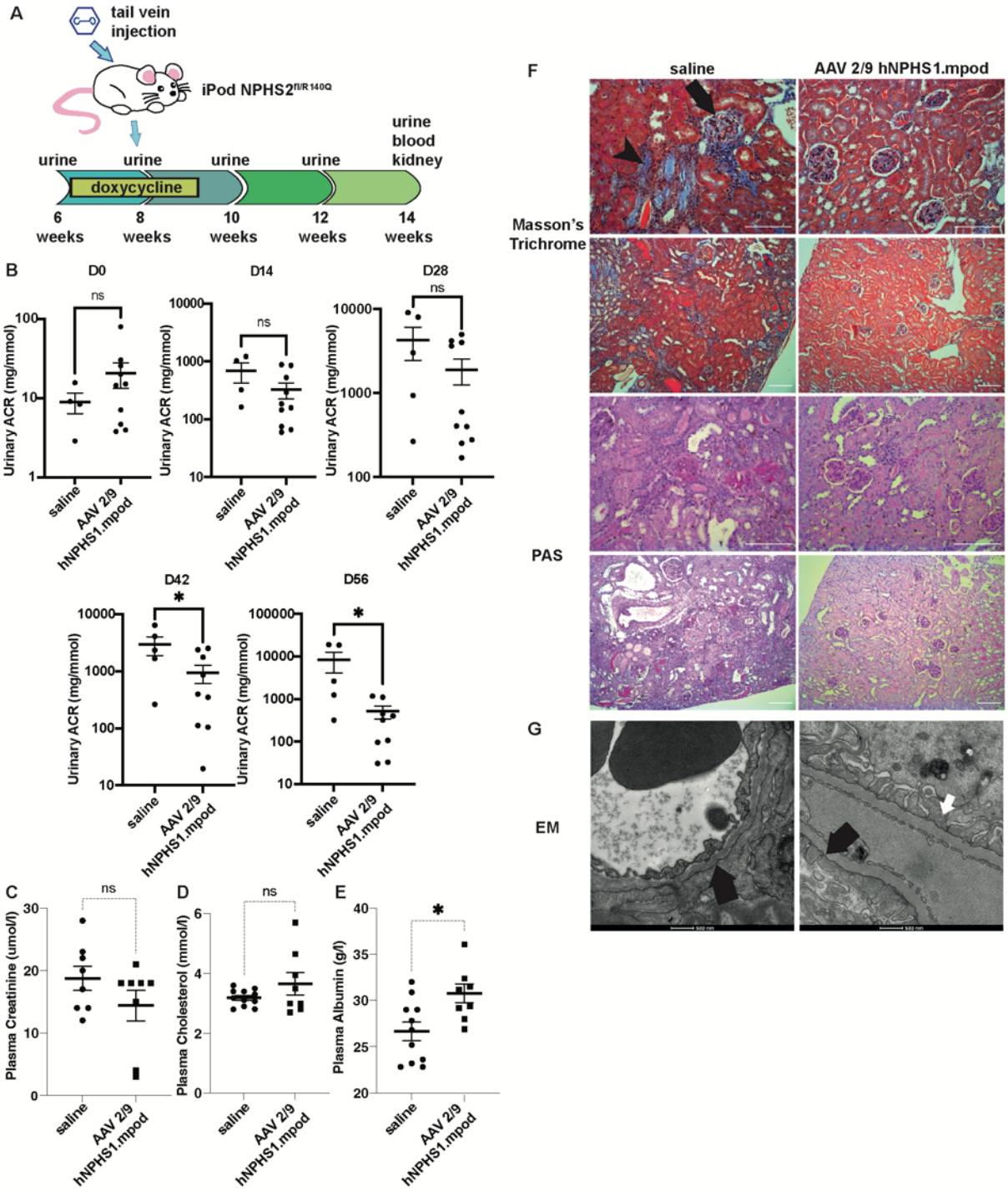

Figure 7. Tail vein injection of AAV 2/9 expressing wild-type podocin under a podocyte-specific promoter after onset of proteinuria reduces proteinuria and improves plasma markers of nephrotic syndrome in the inducible podocin knock-in mouse model (Pod-rtTA TetO-Cre NPHS2$^{fl/R140Q}$). A) Doxycycline was given to 6-week-old Pod-rtTA TetO-Cre NPHS2$^{fl/R140Q}$ mice. Two weeks later, proteinuric mice were injected with vector or

saline via tail vein. Urine was collected every 2 weeks, and mice were culled at 14 weeks of age. B) Urinary albumin: creatinine ratio of saline and vector treated mice every 2 weeks (unpaired T test, * $p<0.05$). Plasma C) creatinine D) cholesterol and E) albumin (unpaired T test, *$p<0.05$) from mice at 56 days after start of doxycycline. F) Representative images on light microscopy. Black arrow indicates glomerulosclerosis while the black arrowhead indicates interstitial fibrosis. Scale bar for light microscopy=100μm. G) Representative images on electron microscopy. Black arrow indicates foot process effacement while white arrow indicates normal foot process appearance. Scale bar for electron microscopy=500nm.

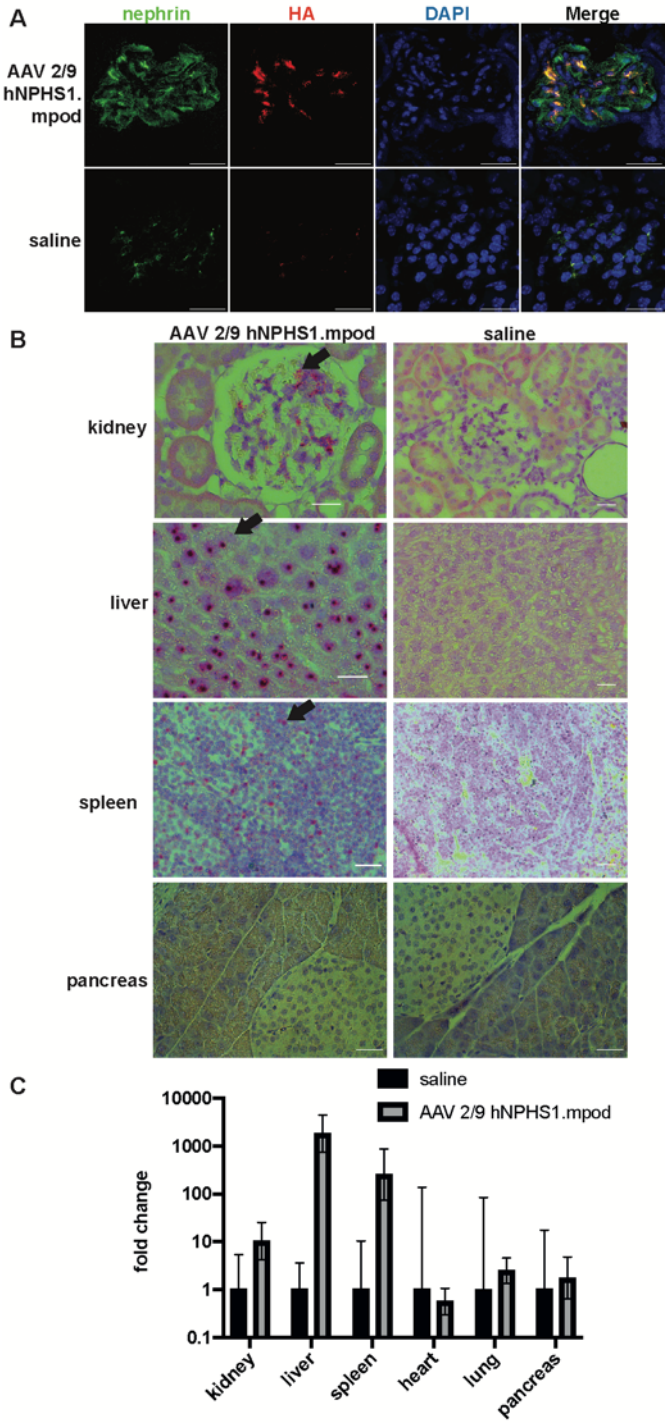

Figure 8. AAV 2/9 hNPHS1.mpod administered by tail vein injection transduces the mouse kidney in inducible podocin knock-in mice (Pod-rtTA TetO-Cre NPHS2$^{fl/R140Q}$), but expression is not limited to the kidney. A) Representative immunofluorescence showing expression of HA (red)-tagged podocin with podocyte-specific protein nephrin (green) in Pod-rtTA TetO-Cre NPHS2$^{fl/R140Q}$ mice injected with either AAV 2/9

hNPHS1.mpod or saline. Nuclei are stained blue. B) RNAScope with an anti-sense probe against WPRE demonstrated the presence of transcripts in kidney glomerulus, liver and spleen. The black arrow indicates the presence of transcripts (bright pink dots). (Scale bar=25μm) B) Real time-PCR of HA-tagged *NPHS2* mRNA in mouse kidney, liver and spleen. (n=3)